

Spatially distributed urban Precipitation-Runoff modelling for a small stormwater catchment

Teklu T. Hailegeorgis*¹ and Knut Alfredsen²

¹ Postdoctoral fellow, Department of Civil and Environmental Engineering, Faculty of Engineering Science and Technology, NTNU, Norwegian University of Science and Technology, S.P. Andersens vei 5 (Valgrinda), N-7491, Trondheim, Norway. tekhi09@gmail.com.

² Professor, Department of Civil and Environmental Engineering, Faculty of Engineering Science and Technology, NTNU, Norwegian University of Science and Technology, S.P. Andersens vei 5 (Valgrinda), N-7491, Trondheim, Norway. knut.alfredsen@ntnu.no.

*Corresponding author (e-mail: tekhi09@gmail.com, [+47] 45069384).

Summary

Better estimation of urban floods is required for reliable design and management of urban water infrastructure, and flood risk assessment. We conducted calibration and evaluation of a spatially distributed Precipitation-Runoff (P-R) model (25m² grids) and 2min temporal resolution for four events (E1-E4) and three seasons: Summer-Autumn (SA1) and snow-influenced Winter-Spring (WS1 and WS2) for a small (21.255ha) stormwater catchment in Trondheim City. We modelled the dominant surface and subsurface (soil moisture and groundwater) components of the urban precipitation water cycle and flow routing.

The calibration resulted in good performance measures (Nash-Sutcliffe efficiency, NSE = 0.65-0.94) and acceptable validation NSE for the seasonal and snow-influenced periods. The infiltration excess surface runoff dominates the peak flows while the QTsubsurface, which is a part of the total subsurface runoff volume (QTsubsurface) contributing to the flow in the sewer pipes, also augments the peak flows. Based on the total volumes of simulated flow

in sewer pipes (Q_{sim}) and precipitation (P) during the calibration periods, the Q_{sim}/P are 21.44% (E1), 51.67% (E2), 31.59% (E3), 23.67% (E4), 17.83% (SA1), 56.50% (WS1) and 53.15% (WS2), which are in close agreement with the results from observed volumes (Q_{obs}/P). The lowest percentage of precipitation volume that is transformed to the total simulated runoff in the catchment (Q_T) is 79.77% (E4) while the water balance showed that the maximum percentage of evapotranspiration loss (ET) and increase in the total catchment storage is only about 20%. The ET/P is less than 3% for E1-E4, WS1 and WS2 while it is about 18% for the warmer season SA1. Therefore, the lower Q_{sim}/P is mainly attributed to the lower $Q_{Tsubsurface}/Q_{Tsubsurface}$, for instance, only 7% (E4), 19% (E1 and SA1), 23% (E3), 30% (WS1), 40% (E2) and 47% (WS2). However, the $Q_{Tsubsurface}$ are markedly higher than the total surface runoff volume ($Q_{Tsurface}$) for some cases (e.g. E1, E2 and SA1). The peakiest flow rates correspond to the WS1. Therefore, urban runoff simulation for sizing of the sewer pipes and flood risk management should include the interactions between the subsurface runoff and flow in sewer pipes, and snow-influenced seasons (in cold climate).

Key words

Calibration and validation; Spatially distributed; Precipitation-Runoff modelling; Source-to-Sink flow routing; Stormwater sewer; Risvollan

Introduction

Increasing trends of world population (e.g., United Nations, 2010) and hence land use modification due to urbanization (e.g., DeFries and Eshleman, 2004) indicate that there is a need for sustainable design and management of urban water infrastructure. Urbanization affects the hydrology of urban catchments and hence urban water management related to urban flooding and safety of humans and infrastructure, risks of pollution of ground water and receiving surface water bodies from leakage and overflow of sewer systems. However, the impacts of urbanization on the different components of urban hydrologic cycle is complex (see

Delleur, 2003). Several studies investigated the major impacts of urbanization on runoff such as increase in runoff peaks, runoff volume and runoff ratio (e.g., Cheng and Wang, 2002; Shuster et al., 2005; Burns et al., 2005; Dietz and Clausen, 2008; Valtanen et al., 2014; Guan et al., 2016), change in hydrological regimes (e.g., Braud et al., 2013), increase in flow velocity and hence decrease in runoff response time due to increase in impervious surfaces and “hydraulically efficient” stormwater drainage pipes (Burns et al., 2005), effects on the long-term groundwater recharge and water balance (Haase, 2009; Barron et al., 2013), decrease in base flow (Lee et al., 2008; Hamel et al., 2013), alteration in water quality of receiving water bodies due to runoff from paved surfaces, stormwater plumes and combined sewer overflows (e.g., water temperature: Herb et al., 2009; nutrients and toxicants: Owens and Walling, 2002; Walsh et al., 2005). Jacobson (2011) suggested that integration of current fields of research are needed to enhance our understanding of the changes which urbanization bring to urban catchments, and to facilitate the development of planning strategies to minimize the negative impacts of future urban growth.

Statistical analyses of the systematic records of extreme precipitation and run off events are commonly employed for determination of the magnitudes and frequency of design storm and design flood for sizing of urban water infrastructure under several sources of uncertainties (e.g. see Hailegeorgis and Alfredsen, 2017). However, statistical models do not allow investigation of the hydrological processes prevailing in extreme runoff generation, how the quantity of generated runoff in urban catchments is affected by catchment soil moisture and groundwater storage states, performances of different source control stormwater management strategies in terms of water quality and quantity, assessment of the impacts of land use and climate change on the runoff quantity and quality, two-way interactions between sewer networks and subsurface flows, etc. Moreover, long runoff records, which are important for reliable statistical analyses are not commonly available in urbanizing catchments. Reliable estimation of runoff is required for design of stormwater systems, and “end-to-pipe” and

source-control (Freni et al., 2010) stormwater management techniques. Fletcher et al. (2013) studied the considerable impacts of urban hydrology on receiving waters and noted that the variability and complexity of rainfall-runoff response in urban areas needs further research. Therefore, better understanding of the dominant urban hydrological processes and runoff generation from rainfall and snowmelt events for different land cover, precipitation characteristics (e.g., intensity, duration, volume, snowfall, rainfall, etc.) and catchment wetness states by using Precipitation-Runoff (P-R) models is crucial for improved decision support in design and management of urban water infrastructure. However, calibration and evaluation of the urban P-R modelling is challenging and requires thorough studies in different urban setting and climate regimes mainly due to:

- i. Urban catchments and urban water cycle are highly complex and heterogeneous due to the anthropogenic impacts such as modification in land cover, soil properties, flow paths, etc., and hence urban P-R modelling require high-resolution spatial information in order to consider the spatial variability of pluviometric and physiographic characteristics;
- ii. Increase in runoff response or flashiness of urban catchments resulting from marked increase of impervious surfaces and alteration from the natural hydrological pathways to “hydraulically efficient” artificial drainage require simulation of rainfall-runoff dynamics in urban catchments from high temporal resolution and good quality hydro-climatic records;
- iii. Lack of complete knowledge on the effects of various urban hydrological processes on the generated runoff volume such as snowmelt, evapotranspiration and two-way interactions between the subsurface runoff and flow in the sewer pipes.

Several urban hydrological model models have been developed for runoff simulation in terms of both quantity and quality in urban catchments (see a review by Elliott and Trowsdale, 2007). Probably being an open source and its suitability for a wide ranges of applications, the

semi-distributed Storm Water Management Model (SWMM) (Huber and Dickinson, 1988; Rossman, 2004) is a widely applied model in literature (see Rossman et al., 2005) for event or continuous runoff simulation (e.g., Denault et al., 2006; Krebs et al., 2014; Guan et al., 2015, Guan et al., 2016). However, some studies reported that there are a number of uncertain parameters in the model and some parameters have no physical meaning (e.g., Krebs et al., 2014; Guan et al., 2015; Guan et al., 2016), the model cannot adequately capture the spatial distribution of runoff contributing areas from the spatially heterogeneous urban catchments due to its semi-distributed parameterization (e.g., Balascio et al., 1998). Zoppou (2001) reviewed urban storm water models and noted that the spatial and temporal variability in rainfall is not adequately considered in the urban stormwater models. Elga et al. (2015) reviewed hydrological modelling of urbanized catchments and suggested that future urban models should consider spatial-temporal variability, process interactions, flexibility and uncertainty reduction. The authors reported that only about 36% of the analyzed modelling approaches are spatially distributed with spatial resolution ranging from 3m to 10km. However, fully distributed models where the model parameters and runoff routing are distributed would entail more complexity and overparameterization. Such models may be useful for special research purposes but may not be useful for practical application for design and management purposes (e.g., see Grayson et al., 1992; Brooks et al., 2007).

Spatially distributed models would allow explicit representation of the grid-to-grid variability of land cover information opposed to the semi-distributed models, which represent the spatial variability of the land cover in terms of percentages of impervious and pervious areas of the sub-catchments or the homogeneous units (HU). Because of the spatially heterogeneous nature of urbanized watersheds where the land cover are varying at a fine spatial scale, distributed models are required to characterize the distribution of hydrologic processes (Easton et al., 2007). The spatially distributed models are more responsive to changes in catchment characteristics and are useful for scenario studies like the impacts of land cover and

climate change on urban runoff generation and on the urban water cycle in general. Cuo et al. (2008) applied a physical based distributed Hydrology-Soil-Vegetation Model (DHSVM) for urban catchment and reported that the model facilitate prediction and/or reconstruction of a range of historic and future changes in land cover due to urbanization or other factors. Rodriguez et al. (2000) evaluated a distributed model for urban catchments using a 7-year continuous data series and found that the model provides a correct description of the temporal variations in the runoff coefficient. Mejía and Moglen (2010) illustrated the influential effects of the spatial distribution of imperviousness on the hydrologic response of an urbanizing basin. Jacobson (2011) found that the distribution of imperviousness within urban areas is important in understanding the impacts of urbanization and quantification requires detailed characterization of urban areas. Petrucci and Bonhomme (2014) based on simulation of runoff quantity and quality using the semi-distributed SWMM model and different representation of spatial variability by increasing use of geographical information found that the land use classification provides the highest benefit to improve model performances.

The spatially distributed models are also suitable for using spatially distributed rainfall input like radar rainfall data (e.g., Pan et al., 2012, a review paper by Thorndahl et al., 2017) or for spatial interpolation of climate forcing from point gauge measurements. The models also allow for distributed simulations of urban water storage states such as surface depression storage, soil moisture and groundwater, and fluxes such as infiltration, evapotranspiration and runoff, for instance, for modelling of runoff and pollutant production from variable source areas (e.g., Easton et al., 2007). The spatial variability of both rainfall and catchment soil moisture state affect urban runoff generation and hence studying the effects of antecedent soil moisture on urban runoff generation is important. In addition, spatially distributed simulations of snow accumulation and melt processes is useful for urban P-R modelling in cold regions.

Urban P-R modelling based on high temporal resolution is also important due to quick runoff response of urban catchments related to modification of land cover (e.g., increase in

imperviousness), relatively small catchment size, high velocity of flow in conduits and high spatial variability of precipitation excess. A review by Elga et al. (2015) identified that the most time steps used for urban runoff simulation are 1h (25%) and 1day (20%), which limit the models from accurately characterizing the fast components of urban fluxes. However, Schilling (1991) recommended rainfall data requirements for urban hydrology application for proof, evaluation, analysis and operation of sewers, at a temporal resolution of less than 5 min and spatial resolution of $\leq 1\text{km}^2$ per gauge. For a Mediterranean climate, Berne et al. (2004) suggested that, the required resolution for rainfall measurements is about 1min and 1.5km, and about 2min and 2km respectively for catchments smaller than 10ha and the order of 20ha. Bruni et al. (2015) based on rainfall rates derived from X-band dual polarimetric weather radar noted that temporal resolution aggregation of rainfall inputs resulted in time shift in modelled flow peaks by several minutes. However, the authors reported that the sensitivity to temporal resolution of rainfall inputs was low compared to that of the spatial resolution. Ochoa-Rodriguez et al. (2015) investigated critical rainfall resolutions for urban catchments to properly characterize catchment response using nine storm events measured by X-band dual polarimetric weather radar and found that for drainage areas between 1ha and about 100ha, rainfall inputs at a spatial resolution of 500m appear to be sufficient while acceptable hydraulic performance is still obtained for rainfall estimates at 1km and 1min resolution. Therefore, hydro-climatic input data and runoff simulation at high temporal resolution (e.g., less than the time of concentration of the catchment and response times of the sub-catchments) is very important for better understanding and prediction of the runoff response in urban catchments.

In addition to the infiltration in pervious areas and infiltration excess runoff from impervious areas, other processes such as surface depression storage, evapotranspiration and snow accumulation and melt influence the urban water cycle. However, Ragab et al. (2003) found that 6%–9% of rainfall infiltrates through paved road surfaces. Previous studies (e.g., Marsalek, et al., 2007; Fassman-Beck et al., 2013) found that there is a variability in the amount

of surface depression water storage capacity and the process of depressing filling in natural surfaces and impervious surfaces including roofs. Several studies (e.g., Grimmond and Oke, 1991; Rodriguez et al., 2008) illustrated that there is a need for better estimation of hydrological fluxes from the surface to the atmosphere (evapotranspiration) in urban areas. Quantifying urban evapotranspiration is imperative to closing the urban water balance, and has implications for the design of stormwater retention and infiltration strategies, along with management of irrigation and the urban landscape (Fletcher et al., 2013). Ragab et al. (2003) found that 21–24% of annual rainfall evaporates. Ramier et al. (2011) found that evaporation losses represent 20% of the total rainfall.

Several studies (e.g., Valeo and Ho, 2004; Bengtsson and Semádeni-Davies, 2011; Moghadas et al., 2015) have discussed the importance of modelling the snow-accumulation and melt processes in urban catchments in cold regions. On their critical review of the evolution of the design storm event concept, Watt and Marsalek (2013) suggested that there might be two drainage design events for pipe and storage sizing: a storm rainfall event and a snowmelt plus rainfall event. However, the authors noted that there are several factors affecting the snow modelling in urban catchments related to non-uniformity of snow distribution in urban environments due to urban snow management practices (e.g., the effect of snow ploughing and piling on snow accumulation and melt, the effect of road salt applications on snowmelt from impervious areas), spatial heterogeneities in surface albedo in urban areas, temporal variations in solar radiation, effects of buildings on wind and solar exposure and hence on atmospheric heat exchange and snowmelt rates. Including these processes in an urban snow model would require several input data and lead to a more complex urban snow model. Therefore, evaluation of simplified parameterizations for the spatially distributed modelling of the dominant hydrological processes (e.g. surface depression storage, evapotranspiration and snow accumulation and melt) is important for improved runoff generation in urban catchments.

Fletcher et al. (2013) noted that integrated urban water cycle models that represent feedback mechanisms between all aspects of urban water cycle (e.g., water supply, wastewater and stormwater systems, and precipitation water cycle) remain an important research challenge. Some studies (e.g., Joss et al., 2008; Dirckx et al., 2009; Weiß et al., 2002; Zhu et al., 2016) found that it is important to model at least the entire urban precipitation water cycle by including the subsurface hydrological processes. Joss et al. (2008) found that there is marked feedbacks between the sewer systems and subsurface media or streams related to sewer leakage. Dirckx et al. (2009) and Weiß et al. (2002) found that there is considerable (50-70%) contribution to the dry-weather combined sewer flow (DWF) from groundwater infiltration. Zhu et al. (2016) found that there are feedbacks between the sewer systems and waterways. Using a 2D numerical model to study the interactions between urban soil and sewer, Berthier et al. (2004) found that the soil contributes an average of 14% of the total per-event runoff volume. Based on a physically based distributed 3D hydrologic model coupled with 1D drainage network model, Domingo et al. (2010) modelled a two-way exchange between overland flow and unsealed manholes and open channels, a two-way interaction between groundwater and pipes, and drainage of groundwater to manholes through foundation drains. The authors found that the simulated volumes of surface floods and inflows to the pipe network are higher than those obtained from the traditional 1D-2D procedure. Berg and Byrne (1998) reported that basements were flooded in residential urban areas due to subsurface flow and percolation into the pervious surfaces. Karpf and Krebs (2011) developed a methodology to quantify groundwater infiltration and surface water inflow in to the sewer pipes. However, the authors noted that the method require data which are not commonly available, for instance, the groundwater data. Using a distributed hydrological model, Rodriguez et al. (2008) illustrated the importance of modelling the exchanges between the sewer system and the soil infiltration in to the sewers and noted that the exchange with the saturated zone deserves detailed investigation. Coutu et al. (2012) modelled the transfer of subterranean flow from the soil to

the sewer drainage network. Rodriguez et al. (2008) and Coutu et al. (2012) modelled based on the conceptualization that the total generated subsurface runoff from the catchments draining in to the stormwater drainage network contributes to the flow in the sewer pipes. However, only fractions of the generated subsurface runoff from a catchment connected to a stormwater network would contribute to the flow in the artificial sewer network through cracked pipes since the subsurface runoff would mainly contribute to the natural subsurface drainage and storages. Based on a review of models for low impact urban stormwater drainage, Elliott and Trowsdale (2007) concluded that half of the models include a groundwater component, which is relevant for assessing effects of LID on baseflow, but the representation of groundwater is simplified and generally untested. However, simplified modelling of urban subsurface runoff process would be useful to shed lights on the total magnitudes of subsurface runoff and interactions between the subsurface runoff and sewer pipes.

Runoff routing is also very important for urban catchments due to the quick rainfall-runoff response in urbanized catchments (e.g., see Lhomme et al., 2004; Rodriguez et al., 2003, 2005a). Miller et al. (2014) noted that runoff routing via a storm drainage network significantly affects the hydrological response of a catchment to storm events. Several overland flow and sewer flow routing methods of different complexity have been developed for urban catchments such as non-linear reservoir method (Xiong et al., 2005), travel time based methods (e.g., urban unit hydrographs: Rodriguez et al., 2003; Urban Morpho-climatic Instantaneous Unit Hydrograph: Gironás et al., 2009), hydraulic routing based on approximate analytical solutions of the diffusive wave model (e.g., Muskingum-Cunge method: Rodriguez et al., 2008; flow path response function based: Mejia and Moglen, 2010; Cantone and Schmidt, 2011) and coupled 1D sewer hydraulics and 2D overland flow hydrodynamic routing based on numerical solution of 1D/2D De Saint Venant equations by explicitly providing a flow path for every grid in the catchment for inundation studies (e.g., see Barnard et al., 2007; Paz et al., 2011). Mays (2001) describes the diffusive wave model as the most useful among the approximations of the

dynamic wave equation, because it offers a balance between accuracy and simplicity for a large number of field situations. Borah (2011) suggested that models using approximate equations with analytical solutions may provide a balance between complexity and accuracy. Therefore, evaluation of the performances a distributed P-R model would be possible based on coupling to a simple runoff routing algorithm without including detailed sewer hydraulics.

Contingent on availability of long hydro-climatic records, continuous hydrologic simulation based on seasonal, long-term or several concomitant extreme precipitation and runoff events are necessary for temporal validation (evaluation) of models, better understanding of precipitation-runoff processes and improved decision making in design and management of urban water infrastructure. Fletcher et al. (2013) noted that continuous simulation is required in order to have an appraisal of the impact of urbanization on the components of the urban hydrological cycle and hydrological regime (e.g., high, medium and low flows) and to predict consequences for water quality. However, literature on temporal validation of urban P-R models and tests for parameter transferability in time are not common and hence needs to be conducted.

The main objectives of the present study are:

- (i) Calibration and evaluation (validation) of the performances of a fine resolution spatially-distributed modelling of the hydrological processes dominating the urban precipitation water cycle (e.g., surface depression storage, infiltration, infiltration excess surface runoff, evapotranspiration, snow accumulation and melt, subsurface runoff, etc.) using ground based observations of hydro-climatic variables in a small urban stormwater catchment;
- (ii) To estimate the effects of soil moisture and groundwater states pertinent to net contributions of subsurface runoff to peak flows in sewer pipes based on calibration of the P-R model; and

- (iii) To investigate the impacts of snowmelt in generating peak flows in sewer pipes during winter and spring (WS) seasons.

Study catchment and data

The study site is a Risvollan research catchment, which is located about 4 km southeast of the center of the city of Trondheim in mid-Norway (Figure 1). The catchment drains a separate stormwater catchment of about 21.255ha (0.21255 km²) urban residential area. In the present study, we subdivided the catchment in to 54 sub-catchments ranging in size from 0.08ha to 1.54ha that are linked by a drainage network (Figure 1). The sewer network contains 78 manholes that are linked to 78 stormwater pipes (conduits) conveying the flow to the outlet (Figure 1). The catchment has one gauging station near the outlet for each precipitation P (mm), air temperature T_a (°C), solar radiation SR_{in} (W/m²), wind speed (m/s) and relative humidity RH_p (%) that are measured at two meters above the ground (Figure 1). The precipitation gauge is an unshielded Lambrecht tipping bucket having a heater when air temperature drops below freezing. It records 0.1mm of precipitation per tip. The catchment receives precipitation mainly in the form of rainfall during May to September and mainly in the form of snowfall during November to March. The mean annual precipitation for the catchment is about 985mm.

We used a climate data that are available at a temporal resolution of 2min, which agrees with the suggestions by Schilling (1991) and Berne et al. (2004) for catchments with an order of 20ha. We used climate data from the only available climate station within the 21.255ha catchment, which is better than gauge densities of 1km² per gauge and 2km spatial resolution that was suggested appropriate respectively by Schilling (1991) and Berne et al. (2004). Due to the availability of only one climate station and the small size of the catchment, we assumed uniform (homogeneous) fields of precipitation and other climate variables over the catchment. A 1-min resolution discharge records were obtained from the Norwegian water and energy directorate (NVE). The 1-min discharge data was converted to 2-minutes resolution to match with the climate data. Then a simulation time step of 2-min was used. Due to considerable

missing climate or flow records, we selected calibration periods having no missing records of climate data and with relatively low missing flow records comprising four events (E1 to E4), Summer-Autumn season (SA1) and two Winter-Spring (snow-influenced) seasons (WS1 and WS2) from 1993 to 1998 for parameter calibration and validation. The percentages of missing flow records for E1, E2, E3, E4, SA1, WS1 and WS2 are respectively 1.1%, 0.79%, 1.94%, 11.2%, 1.37%, 1.97% and 0.23%. The maximum observed precipitation volume (mm) at the 2 min aggregation time are 1.5 (E1), 0.5 (E2), 0.3 (E3), 0.4 (E4), 0.6 (SA1), 1.4 (WS1) and 0.3 (WS2). The ranges of observed air temperature (°C) are 10.9-12.7 (E1), 2.9-8.6 (E2), 7.1-11.0 (E3), 11.2-18.9 (E4), -7.2-28.9 (SA1), -19.8 - 9.3 (WS1) and -20.7 - 8.8 (WS2) while the temperature records below freezing for the SA1 occurred only for a short period. The maximum (peak) observed flow in the sewer pipes (ls^{-1}) are 216.6 (E1), 152.7 (E2), 140.1 (E3), 130.3 (E4), 140.1 (SA1), 432.34 (WS1) and 206.5 (WS2) while the peak observations may be missing especially for the calibration periods with higher proportions of missing records.

The ground elevation of the catchment ranges from 85 to 134masl. In the present study, based on a land use or land cover map (Figure 1), 22.5% of the catchment area (14% roofs or buildings and 8.5% paved roads) are considered impervious. The remaining (77.5%): 41% open areas including grassland, 35% built-up areas (e.g., lawns, walkways, parking spots, playgrounds, etc.) and 1.5% vegetation or trees are considered as pervious surfaces. We used a 5mx5m grid to represent the spatial variability of land cover, and hence for spatially distributed simulation of state variables, runoff and other fluxes accordingly.

Methods

The P-R model used in the present study comprises of potential evapotranspiration (PET) model, snow accumulation and melt model (Snow), runoff response model (RR) and a runoff routing model based on the Source-to-Sink (STS) algorithm. The model structure for the runoff generation is given in Figure 2.

Potential evapotranspiration (PET) model

Several urban surface energy balance models of different complexity and data requirements (e.g., climate forcing data, urban morphology, surface properties, anthropogenic heat sources, etc.) are available in literature (see a review by Grimmond et al., 2009). In the present study, we used a simple approach based on the Priestley-Taylor method (Priestley and Taylor, 1972) for the calculation of potential evapotranspiration, PET (mm). The method uses solar radiation, air temperature and relative humidity climate forcings and considers surface properties including albedo, emissivity and temperature:

$$PET = \alpha \frac{\Delta}{\Delta + \gamma} (R_n - Q_g) \left(\frac{\Delta t}{\lambda_v} \right), \quad (1)$$

where the α is the Priestley-Taylor coefficient, λ_v is the latent heat of vaporization of water ($\lambda_v = 2501000 - 2361T_a$ in kJ/m^3) and Δt is simulation time step (s). The net radiation R_n (W/m^2) is the sum of net shortwave radiation (SR_n) = $SR_{in} - SR_{out}$ and the net longwave radiation (LR_n) = $LR_{in} - LR_{out}$. We estimated the reflected shortwave radiation SR_{out} based on albedos of the snow or land surface ($alb_{s/l}$). We computed the LR_{in} and LR_{out} respectively based on Sicart et al. (2006) and Stefan-Boltzmann equation by considering the atmospheric, snow surface and land surface emissivity. The Δ (Pa/oK) is the slope of saturation vapor pressure of air (e_{sa}) curve. We computed the e_{sa} (Pa) and the Psychrometric constant γ (Pa/oK) respectively based on Koutsoyiannis (2012) and FAO-56 method (Allen, 1998). The Priestley-Taylor constant α and albedo for the land surface alb_l are set by calibration. The snow albedo is set as a state variable, which varies with snow age and decays slowly during cold conditions ($T_a < 0$) and decays fast during melt ($T_a > 0$) respectively modified from Baker et al. (1990) and Verseghy (1991), for instance, as implemented in the Gamma distributed snow depletion curve model (see Hegdahl et al., 2016):

$$alb_s(t+1) = \begin{cases} alb_s(t) - \frac{0.5(alb_{max} - alb_{min})\Delta t_d}{dc_s}, T_a \leq 0 \\ (alb_s(t) - alb_{min})2^{\frac{-\Delta t_d}{dc_f}} + alb_{min}, T_a > 0 \end{cases}, \quad (2)$$

where alb_{max} is maximum snow albedo (= 0.93 was used), alb_{min} is minimum snow albedo (= 0.10 was used following Mathuesen, 2004), Δt_d is the simulation time step in days, and dc_s and

dc_f respectively are albedo decay rates respectively in cold conditions and during melt in days

(d). The snow albedo was set to increase during snowfall ($S_n > 0$) by $\frac{alb_{range}}{alb_{res_d}}$, where $alb_{range} = alb_{max} - alb_{min}$ and alb_{res_d} is a snowfall depth after which the snow albedo is reset to a fresh snow albedo and was determined by calibration. We partitioned the precipitation P (mm) in to snowfall S_n (mm) and rainfall R (mm) based on the air temperature T_a , threshold temperature for 100% precipitation falling as rainfall T_r and threshold temperature for 100% precipitation falling as snowfall T_s following Tarboton et al. (1994). The T_r and T_s are determined by calibration. The Q_g (Wm^{-2}) is the ground heat flux at the surface and the upper layer of soil estimated as:

$$Q_g = -K_{th}(T_{soil} - T_{sur})D_{soil}, \quad (3)$$

where K_{th} is the thermal conductivity ($Wm^{-1}C^{-1}$), T_{soil} is soil temperature ($^{\circ}C$), D_{soil} (m) is effective soil depth for the heat transfer and T_{sur} is the surface temperature ($^{\circ}C$). The K_{th} and D_{soil} , are determined by calibration. The surface temperature (T_{sur}) is defined as a snow surface temperature T_{Sn} when the snow covered area (SCA) > 0 and by a land surface temperature T_l when the SCA = 0. Using empirical linear regression relationships, the snow surface temperature was estimated from the dew temperature following Raleigh et al. (2013), and the land surface and soil temperatures were estimated from an air temperature following Gallo et al. (2009). To reduce the numbers of calibrated parameters, the values of slope parameters are set to one while the intercept parameters are determined by calibration. There are 12 calibrated parameters in the PET model (Table 1).

Snow accumulation and melt model

There are three main snowmelt models in literature namely temperature index or degree-day model, energy balance models having one or more snowpack layer, and combination of the two as hybrid models (see a review by Moghadas et al., 2015). Some P-R models (e.g., HSPF model: Bicknell et al., 2001; HBV light model: Seibert, 2002) used the simplest snow model known as the temperature index model. Based on study on the sensitivity of modelled

discharge of different snowmelt parameterizations (temperature index to energy balance methods) for the Himalayan region, Hegdahl et al. (2016) found that model performance is more sensitive to the precipitation input than to the choice of snowmelt routine. In the present study, we used the degree-day based model that includes parameterization of sub-grid heterogeneity of snow cover by a statistical distribution (Tøfte and Kolberg, 2016). The method is similar to the snow routine of the Hydrologiska Byråns Vattenballansavdelning or HBV model (Bergström, 1976) but does not involve elevation zones within each grid cell rather the snow cover percentages of the spatial grid cell is defined by a statistical distribution described by five quantiles (00, 25, 50, 75 and 100), which makes the snow cover in a grid cell to vary between 0 and 100%. Each quartile has three state variables namely snow water equivalent (SWE), liquid water content of the snow pack and the SCA. The model requires inputs of precipitation and temperature time series, simulates refreezing and melting, and provides distributed water release from snowpack (snowmelt + rainfall) as an output. There are 10 calibrated parameters in the snow model including five snow redistribution weights for each quartile (Table 1).

Runoff response model (RR)

Surface depression storage, evapotranspiration, infiltration and infiltration excess surface runoff

In the present study, we conceptualized the catchment as three storage reservoirs (surface depression, soil moisture and groundwater), each characterized by a state variable representing their respective water storage. We considered the roofs (buildings) and paved roads as impervious surfaces assuming a negligible infiltration following Petrucci and Bonhomme, (2014) even if Ragab et al. (2003) reported that 6%–9% of rainfall infiltrates through paved road surfaces and Rodriguez et al. (2008) reported that 11.6% of precipitation infiltrates through streets. Therefore, for the impervious surfaces, only the surface runoff generation processes (i.e. surface depression storage, actual evaporation from the surface depression storage, snow processes and infiltration excess surface runoff) are modelled. For the

impervious surfaces, the subsurface runoff processes are neglected and hence there is only one state variable namely the surface depression storage.

We updated the surface depression storage (h) after consecutively updating fluxes of snow outflow (S_{of}), actual evaporation from the surface depression storage (AE), infiltration to the unsaturated soil (I) (for pervious areas) and infiltration excess surface runoff (I_{excSF}):

$$h_t = h_{t-1} + S_{of} - AE - I - I_{excSF}, \quad (4)$$

The actual evaporation from the surface depression storage was computed from the potential evapotranspiration and surface depression storage (e.g., Rutter et al., 1971; Rodriguez et al., 2008) by parameterizing with a maximum surface depression storage parameter after which the actual evaporation occurs at a potential rate (h_{maxPET}). Several algorithms are available to estimate infiltration rates, for instance, the Green-Ampt method (e.g., Green and Ampt, 1911; Camici et al., 2011), Horton's infiltration flux (e.g., Horton, 1940; Coutu et al., 2012), Philip's infiltration equation (e.g., Philip, 1957; Stewart et al., 2013) and based on parameterizing by the maximum infiltration capacity. In the present study, we limited the infiltration flux from pervious areas either by the soil maximum infiltration capacity i_c (mm/h) parameter or by the surface depression storage h . The i_c was calibrated separately for open areas and vegetation or trees (i_{cp}), and built-up areas (i_{cb}). Several algorithms are available for computation of the infiltration excess surface flow (I_{excSF}), for instance, based on the Manning's equation (Singh and Aravamuthan 1996; Du et al., 2009), linear reservoir flow from surface depression storage (e.g., Coutu et al., 2012) and threshold capacity for surface depression storage (e.g., Rodriguez et al., 2008). In the present study, we computed the I_{excSF} based on a threshold maximum depression storage capacity parameter h_{max} after which the infiltration excess surface flow occurs following Rodriguez et al. (2008). The h_{max} was calibrated separately for open areas and trees or vegetation (h_{maxPer}), built-up areas (h_{maxBu}) and impervious areas (h_{maxImp}). We neglected interception and evaporation from interception due to only small proportion (1.5%)

of the vegetation or trees in the catchment and lower magnitudes of fluxes associated to these processes in urban catchments (e.g., see Rodriguez et al., 2008).

Subsurface runoff and saturation excess surface runoff

In the present study, we modelled the interflow (runoff from the soil moisture), percolation from soil moisture to groundwater (*Perc*) and groundwater flow (*GF*). We updated the soil moisture storage (*SS*) and ground water storage (*GS*) state variables by consecutively updating the fluxes based on the following water balance equations:

$$SS_t = SS_{t-1} + I - Perc - AET - IF \quad (5)$$

$$GS_t = GS_{t-1} + Perc - GF, \quad (6)$$

We computed the actual evapotranspiration from the soil zone *AET* (mm) as:

$$AET = (PET - AE)S_r; S_r = \frac{\theta - \theta_r}{n - \theta_r}, \quad (7)$$

where the S_r is the degree of soil saturation, θ (-) is the initial volumetric soil water content, θ_r is residual soil moisture content and n is soil porosity. The θ_r and n are parameters determined by calibration. To compute the percolation, we used the van Genuchten soil moisture characteristics functions (van Genuchten, 1980), which is based on the S_r , saturated hydraulic conductivity K_{sat} and the soil pore-size index m . We computed the interflow from soil moisture (*IF*) and groundwater flow (*GF*) based on conceptualizing the soil moisture storage and groundwater storage as linear reservoirs (e.g., Coutu et al., 2012):

$$IF = k_{soil}SS\Delta t, GF = k_{gw}GS\Delta t \quad (8)$$

We parametrized net fractions of the interflow and groundwater flow entering the sewer pipes through cracks as effective (calibrated) parameters respectively denoted as p_{in} and p_{dr} . We used the term net fraction since two-way interaction i.e. both infiltration to the pipes and exfiltration from the pipes may occur. However, we assumed that infiltration to the pipes is higher than exfiltration from the pipes. We computed the total runoff from the grid cell entering the stormwater sewer (T_F) in mm as:

$$T_F = I_{exSSF} + S_{exSSF} + IF_{sewer} + GF_{sewer}; IF_{sewer} = p_{in}IF; GF_{sewer} = p_{dr}GF, \quad (9)$$

where the k_{soil} (s^{-1}), k_{gw} (s^{-1}) are parameters determined by calibration. Saturation excess surface flow (S_{exsSF}) from pervious grids occur when the $SS > SS_{max}$ or the total subsurface storage $TS = SS + GS > TS_{max} = SS_{max} + GS_{max}$. The GS_{max} and TS_{max} respectively are the maximum ground water storage and total subsurface storage capacities, which are set as effective parameters and determined by calibration. There are 16 calibrated parameters in the RR model (Table 1).

Runoff routing model

In the present study, we used the flow path response function based on an analytical solution to the diffusion wave equation (Hayami, 1951; Nauman, 1981) to route the generated runoff from the grid cells (sources) to the outlet (sink) following the source-to-sink (STS) routing algorithm (e.g., Olivera and Maidment, 1999). The total flow travel length for the grid cells is the sum of flow length over the surface before entering the manholes (i.e., flow travel length outside the pipes) and the flow length inside the pipes to the outlet. The flow travel length outside the pipes (FL_{op}) was computed based on sub-catchment area (A_{SC}) and a shape factor (SF) parameter following Guo and Urbanos (2009):

$$FL_{op} = \left(\frac{A_{SC}}{SF} \right)^{0.5}, \quad (10)$$

where the SF was set as an effective (calibrated) parameter used for all sub-catchments. The FL_{op} for the sub-catchments were used for all grid cells in the sub-catchments i.e. the same entry time to the conduits is assumed for all grid cells within the sub-catchment. The total flow travel time for each grid cell to the outlet was obtained by summing the travel time for the surface flow (or the entry time) and flow travel time inside the sewer pipes. If spatially and temporally invariant celerity and dispersion coefficient are assumed, the instantaneous runoff generated at the source are related to the outlet response by a unit flow path response function or $U_i(t)$ [$1/T$] (see Olivera and Maidment, 1999; Hailegeorgis et al., 2015):

$$U_i(t) = \frac{1}{2t \sqrt{\frac{\pi(\frac{t}{T_i})}{\Pi_i}}} \exp\left(-\frac{[1 - (\frac{t}{T_i})]^2}{\frac{4(\frac{t}{T_i})}{\Pi_i}}\right), T_i = \frac{FL_{op}}{V_{op}} + \frac{FL_p}{V_p}, \Pi_i = \frac{FL_{op}V_{op}}{D_{op}} + \frac{FL_pV_p}{D_p}, \quad (11)$$

where the L_{op} and L_p respectively are flow travel lengths over the surface and inside the pipes, the V_{op} and V_p respectively are velocities of surface flow and pipe flow, and the D_{op} and D_p respectively are dispersion coefficients for surface and pipe flows. The flow path response function for a grid cell ‘ i ’ represents the probability distribution of flow travel time (t) from the source (grid cell) to the sink (outlet) with a mean value of T_i . The flow path Peclet number (Π_i) is a representative measure of the relative importance of advection with respect to dispersion where the flow dispersion coefficients represent the effects of storage and spreading. Even though a distributed response function can be computed for each grid cell i , in the present study all the grid cells in a sub-catchment j have the same flow path response function due to assigning the same entry time for all grid cells in a subcatchment j . The velocities of flow and dispersion coefficients are effective parameters determined by calibration. For a spatially distributed linear system subdivided into uniform non-overlapping sub-areas (e.g., Olivera and Maidment, 1999), the runoff routing can be performed by the following convolution:

$$Q_{sim}(t) = \frac{1000}{\Delta t} \sum_{i=1}^N T_{Fvol} \otimes U_i(t), \quad (12)$$

where $Q_{sim}(t)[l/s]$ is a STS routed simulated discharge, N is the total number of grid cells in the catchment, $T_{Fvol}[m^3]$ is the total generated runoff volume during the time step for the grid cell and \otimes is the convolution operator. There are 5 calibrated parameters in the STS flow routing model (Table 1).

Parameter identification

We used a random Monte Carlo (MC) sampling procedure for parameter calibration to identify parameter sets that provide the best performance measure. The performance measure used in the present study is the Nash-Sutcliffe efficiency or NSE (Nash and Sutcliffe, 1970) using the flow in the outlet of the sewer network (Q) as a target variable. Descriptions of the calibrated parameters and their minimum and maximum values for the MC sampling are given in Table 1.

Results

Calibration and validation

Performance of the model in terms of the NSE during calibration and validation periods are given in Table 2. The calibration provided good NSE values ranging from 0.81 to 0.94 for events (E1-E4), 0.76 for Summer-Autumn season (SA1) and respectively 0.65 and 0.81 for Winter-Spring seasons WS1 and WS2. Performance of the model are varying among the validation periods. The NSE values for the validation periods ranges from 0.32 to 0.67, -0.46 to 0.85, -0.31 to 0.67, 0.19 to 0.64 and 0.23 to 0.81 respectively for E1, E2, E3, E4 and SA1. The validation performance is good for some events and the seasonal calibration during the Summer-Autumn season. The NSE values for validation of the snow-influenced seasons WS1 and WS2 are respectively 0.65 and 0.57, which are good performance. The results indicate that simulation of snowmelt dominated runoff and/or using longer records are more validated than runoff occurring from shorter rainfall events. The event E3 (09.06.1995-11.06.1995) and the seasonal SA1 (01.06.1995-01.10.1995) found to be better recipients of the transferred parameters than the other periods which probably show that the 1995 data may exhibit a better quality.

Plots of hydrographs of observed flow (Q_{obs}) and routed simulated flow (Q_{sim}), and some unrouted generated runoff fluxes for the event-based calibrations are given in Figures 3a-d respectively for E1, E2, E3 and E4. Plots of the simulated and observed flow hydrographs along with other variables related to the snow model (for WS1 and WS2) for the seasonal calibrations SA1, WS1 and WS2 respectively are given in Figures 4a-c. Plots of the dominant generated runoff fluxes (unrouted) for SA1, WS1 and WS2 are given respectively in Figures 5a-c. The observed and simulated hydrographs exhibit good agreement. The hydrographs indicate that the urban catchment responds quickly to rainfall or snowmelt events and the infiltration excess surface runoff (I_{exsSF}) is the main runoff generating mechanism contributing to the peak flows. The results also indicate that a subsurface flow from the soil moisture zone or the interflow

(IF) is contributing to the sewer flow IF_{sewer} and augment the peak flows and sustain base flows while the contribution to the peak flows is more relevant to design flood and flood risk management in urban catchments. For instance, the calibrated values of the p_{in} implies that 19%, 40%, 23%, 7%, 19%, 30% and 47% of the IF contributes to the flow in the sewer pipes (IF_{sewer}) respectively for E1, E2, E3, E4, SA1, WS1 and WS2 while the remaining interflow would contribute to the natural subsurface drainage or storage system. Calibration results for the snow seasons (WS1 and WS2) (Figures 4b-c) show that when the observed air temperature is well above freezing (0 °C), there are generally higher values of the snowoutflow (Sof), the SWE recedes and the SCA decreases. The temperature index based snow model underestimates the peak flows for WS2 i.e. the simulated peak flow rate $Q_{simpeak} = 149.9\text{ls}^{-1}$ and the observed peak flow rate $Q_{obspeak} = 206.5\text{ls}^{-1}$ while it overestimates the peakiest flow during the present study very slightly, which corresponds to the WS1 i.e. $Q_{simpeak} = 462.8\text{ls}^{-1}$ and $Q_{obspeak} = 432.3\text{ls}^{-1}$. Therefore, the results indicate that the performance of the snow model is generally good.

Fluxes and water balance

The total observed precipitation and flow, and total simulated volumes of the different fluxes and change in total catchment storage all expressed in mm over the catchment, and ratios of the different fluxes and the precipitation falling over the catchment (%) during the calibration periods are given in Table 3. The total observed precipitation (P) ranges from 16.7mm (E4) to 566.8mm (WS1). The maximum precipitation intensities (mmh^{-1}) during the calibration periods are 45, 15, 9, 12, 18, 42 and 9 respectively for E1, E2, E3, E4, SA1, WS1 and WS2 while the average precipitation intensities (mmh^{-1}) over the calibration periods are 1.56, 0.70, 1.27, 2.09, 0.08, 0.24 and 0.28 respectively for E1, E2, E3, E4, SA1, WS1 and WS2. The simulated runoff at the outlet of sewer pipes (Q_{sim}) ranges from 3.95mm (E4) to 320.24mm (WS1). In the present study, we used the linear interpolation for filling of the missing records for the calibration periods with small proportion of missing flow records (i.e.

E1, E2, E3 and WS2) in order to estimate the total volume of observed runoff (Q_{obs}) at the outlet of the sewer network. For these calibration periods, the Q_{sim}/Q_{obs} ranges from 78.83% (WS2) to 91.92% (E1) indicating that the model underestimates the runoff volume by up to 20%. Probably the underestimation is mainly attributed to the peak flows, for instance, $Q_{obspeak}/Q_{simpeak}$ for the calibration periods E1, E2, E3 and WS2 respectively are 1.15, 1.03, 1.17 and 1.38 indicating that the peak flow rate is underestimated by up to 38%. The $Q_{obspeak}/Q_{simpeak}$ for the calibration periods E4, SA1 and WS1 for which no filling of missing observations were performed and hence the peak flow observations are probably missing are respectively 0.82, 1.04 and 0.93.

The simulated total runoff (QT) ranges from 13.32mm (E4) to 565.06mm (WS1). The differences between the P and QT represent the loss by the total evapotranspiration (ET) and/or contribution to an increase in total storage volume or $\Delta TotS$ (E1, E3, E4 and WS2). However, for E2, SA1 and WS1, there is a decrease in $\Delta TotS$, which contributed to the QT and the ET demand. The total simulated surface runoff ($QT_{surface}$) enters the sewer pipes through the manholes and the calibration provided values ranging from 1.29mm (E1) to 208.55mm (WS1). The total simulated subsurface runoff ($QT_{subsurface}$) volume ranges from 10.08mm (E4) to 356.5mm (WS1) while the volume of subsurface runoff contribution to the sewer flow ($QT_{subsurfacesewer}$) ranges only from 0.71mm (E4) to 107.08mm (WS1). The calibration provided no saturation excess surface flow ($SatexsSF$) and negligible groundwater flow (GF), and hence there is no contribution of the $SatexsSF$ and there is negligible contribution of the GF_{sewer} to the flow in the sewer pipes during all calibration periods.

The percentages of precipitation volume that is transformed to total runoff volume and other fluxes are varying among the calibration periods. The higher percentage of precipitation occurring as $QT_{surface}$ corresponds to the WS1 (36.79%) while the lower corresponds to the SA1 (3.16%). Considerable percentages of precipitation (P) infiltrates and contributes to the $QT_{subsurface}$, for instance, the lower is 60.38% for E4 and the higher is 78.83% for SA1. The

infiltrated runoff volume contributes mainly to the interflow from the soil moisture (unsaturated zone) and negligible amount is percolating to the ground water zone resulting in negligible GF and GFsewer.

The percentage of precipitation that is transformed to the QT is high, for instance, ranges from 79.77% for E4 and nearly 100% for WS1. The lower value for E4 is related to high contribution of the precipitation volume to the increase in the ΔT_{TotS} and the higher value for the WS1 is because of the low evapotranspiration demand during the snow season and runoff contribution from the decrease in the ΔT_{TotS} that is dominated by the snow water equivalent. The percentage of precipitation lost to the total evapotranspiration is less than 3% for the events (E1 to E4) and for snow seasons (WS1 and WS2) while it amounts to about 18% during the summer and Autumn seasons (SA1). The percentage of precipitation volume contributing to the flow in the sewer pipes (Q_{sim}/P) are 21.44% for E1, 51.67% for E2, 31.59% for E3, 23.67% for E4, 17.83% for SA1, 56.50% for WS1 and 53.15% for WS2. The ratios of observed flow and precipitation volumes (Q_{obs}/P) for the calibration periods for which the smaller proportions of missing flow records are filled are 23.32% for E1, 58.94% for E2, 38.17% for E3 and 67.43% for WS2. These Q_{obs}/P results are slightly higher than their corresponding Q_{sim}/P . The higher Q_{sim}/P values are mainly related to the snow seasons due to low evapotranspiration demand and relatively higher contributions to the sewer pipes from both surface and subsurface runoff while the lower value of Q_{sim}/P is related to the warmer Summer-Autumn season having high evapotranspiration loss and low surface runoff contribution. The results indicate that considering the snow, evapotranspiration and surface depression storage processes would be important in sizing of sewer pipes. The Q_{sim}/P values for E1 and SA1 are found to be less than the precipitation volume falling on the impervious surfaces since the percentage of impervious surfaces in the catchment is 22.5% and infiltration was not allowed on the impervious surfaces. This is due to a large actual evaporation loss (AE) from surface depression storage for the SA1 and the precipitation volume contributes to an

increase in surface depression storage volume for the E1 indicating that the impact of depression storage on the runoff volume is high in event-based runoff simulation and the impact of evaporation loss on the runoff volume is high for long-term simulation during warmer seasons.

The percentage of total simulated runoff (QT) contributing to the Qsim ranges from 21.75% (SA1) to 58.49% (WS2) while the higher percentage is related to higher contribution of the QTsubsurface to the Qsim. For most of the calibration periods, for instance, for E1, E2, E3, SA1 and WS2, the percentage contributions of subsurface runoff to the flow in the sewer pipes are found to be higher than the contributions from the surface runoff.

Runoff routing

Plots of mean flow travel times to the outlet for the subcatchments or T_i , which was obtained from the calibrated parameters of velocity of flow outside sewer pipes (V_{op}) and velocity of flow inside sewer pipes (V_p), are given in Figure 6a. The calibration resulted in different values of the mean flow travel time for the sub-catchments with E3 having the largest travel time (slow runoff response) ranging from 3.3min to 29.28min and E4 having the smallest flow travel time (quick runoff response) ranging from 1.74min to 7.03min. The quick runoff response for E4 may be related to the higher average rainfall intensity for E4 but no general trend is observed between either of the maximum or average precipitation intensities, and the flow travel time. Catchments with larger flow travel lengths to the outlet over the surface and inside the pipes exhibit higher mean flow travel time due to parameterizing the flow velocities as effective parameters and hence the same values are applied to all sub-catchments and sewer pipes. The calibration periods also exhibit different runoff delay since the STS response function is dependent on the T_i and the flow path Peclet number (Π_i), which are found to be different among the calibration periods. Plots of typical STS response functions for the WS1 calibration for some subcatchments are given in Figure 6b.

Discussion

Calibration and validation

The NSE performance measure for the event and seasonal calibration periods of 0.65 to 0.94 that are obtained in the present study (Table 2) are better than or within the ranges of the performance measures obtained from calibration of P-R models in urban catchments using flow as a target variable in previous studies (e.g., Berthier et al., 2004: NSE = 0.77; Valeo and Ho, 2004: NSE = 0.12 to 0.74; Rodriguez et al., 2005b: NSE = 0.54; Easton et al., 2007: NSE for the Full Urban Model = 0.71-0.85; Rodriguez et al., 2008: NSE = 0.51 and 0.54; Gironàs et al., 2009: modified coefficient of efficiency or MCE = 0.52-0.82; Mejía and Moglen, 2010: NSE = 0.42-0.96 and Coutu et al., 2012: NSE = 0.73). Thorough validation of urban hydrological models based on transfer of calibrated parameters are not common in previous studies. However, some studies which conducted validation tests reported acceptable validation performance, for instance, Coutu et al. (2012) obtained that the NSE value for three months validation period is in the same range of the NSE values for five months calibration period (NSE = 0.73), Gironàs et al. (2009) obtained that the MCE values for validation based on twelve events are in the range of MCE values for calibration based on five events (MCE = 0.52 to 0.82), and Mejía and Moglen (2010) obtained NSE values of 0.57-0.74 for validation events. In the present study, the validation performance vary among the parameter transfer between the different periods while generally the NSE for the validation periods are good for the snow-influenced (WS) seasons and for long-term (seasonal) calibration than the event-based periods (Table 2). Therefore, the present study indicated that parameter calibration and validation of the P-R models based on long records spanning the entire range of rainfall and runoff in the catchment (peak flow, medium flow, low flow, rainfall dominated runoff, snowmelt dominated runoff, etc.) or continuous simulation are necessary for reliable model evaluation and decision making. Therefore, extensive hydro-climatic measurements are important for urban catchments.

Fluxes and water balance

The observed flow and precipitation records and the corresponding simulations indicated that lower, for instance, as low as 23.32% (for E1) and 17.83% (for SA1) of precipitation volumes are transformed respectively to observed and simulated flow volumes at the outlet of sewer drainage network (Table 3). The simulation indicated that the differences are because of only a lower proportion of the total subsurface runoff ($Q_{Tsubsurface}$) contributes to the flow in the sewer pipes $Q_{Tsubsurfacesewer}$, the precipitation contributes to a marked increase in the water storage volume in the catchment (e.g. for E1) and satisfies the marked evaporation demand during the warm season (SA1). The lowest percentage of precipitation volume that is transformed to the total simulated runoff volume (Q_T) in the catchment of 79.77% corresponding to the E4 (Table 3) indicate that the maximum percentage loss to evaporation and increase in catchment storage is only about 20%. Therefore, the lower volume of Q_{sim} compared to P is mainly attributed to the lower proportion of the total subsurface runoff volume ($Q_{Tsubsurface}$) contributing to the $Q_{Tsubsurfacesewer}$ through cracked pipes: 7% for E4, 19% for both E1 and SA1, 23% for E3, 30% for WS1, 40% for E2 and 47% for WS2. The results of the present study agrees with Berthier et al. (2004) who found that the soil contributes an average of 14% of the total per-event runoff volume, Rodriguez et al. (2008) who found that 29.1% of the precipitation volume contributes to stormwater and wastewater sewer systems and Dirckx et al. (2009) and Weiß et al. (2002) who found that there is 50-70% contribution to the dry-weather combined sewer flow from groundwater infiltration. The results of the present study illustrated that subsurface runoff contribution to flow in sewer drainage network should not be conceptualized in a way that the whole generated subsurface runoff in the stormwater catchment drains to the sewer pipes since only part of the subsurface runoff contribute to the flow in the artificial stormwater sewer network through cracks or joints while the higher proportion of subsurface runoff would drain to the natural drainage or storage system. Parameter calibration of the urban P-R models based on conceptualizing that the total generated subsurface runoff from catchments draining to the stormwater sewer network would contribute

to flow in the sewer pipes (e.g. Rodriguez et al., 2008, Coutu, et al., 2012) may result in overestimation of evapotranspiration loss, and simulated flow volumes and flow rates. Despite only partial contribution of the generated subsurface flow to the sewer pipes was allowed in the present study, there are higher contributions of subsurface runoff to the sewer pipes compared to the surface runoff for most of the calibration periods (Table 3). This indicate that it is important to model the entire urban precipitation water cycle by including the subsurface hydrological processes as suggested in previous studies (e.g., Joss et al., 2008; Dirckx et al., 2009; Weiß et al., 2002; Zhu et al., 2016) to determine the contributions from subsurface runoff to peak flows in sewer pipes for sizing the capacity of sewer pipes and urban flood risk management rather than based on only contribution from the surface runoff.

In the present study, the P-R underestimated the Q_{sim} by up to 20% and the peak flow rate by about 38% (WS2). The highest underestimations are related to winter spring seasons that are dominated by the snow processes, which is probably due to low performance of the snow model based only on air temperature. However, the snow model slightly (i.e. by 7%) overestimated the peakiest flow rate of the present study, which is associated to the WS1 calibration period ($Q_{simpeak} = 462.8 \text{ ls}^{-1}$ and $Q_{obspeak} = 432.3 \text{ ls}^{-1}$). Several studies (Valeo and Ho, 2004; Bengtsson and Semádeni-Davies, 2011; Moghadas et al., 2015) noted that there are several factors affecting the snow processes in urban catchments related to the effects of snow ploughing and piling on snow accumulation and melt, the effects of road salt applications on snowmelt from impervious areas, spatial heterogeneities in surface albedo, temporal variations in solar radiation, effects of buildings on wind and solar exposure and hence on atmospheric heat exchange and snowmelt rates. The observed peak flow rates (ls^{-1}) for the calibration periods with filled missing flow observations E1, E2, E3 and WS2 are respectively 216.6, 152.7, 140.1 and 206.5. The observed peak flow rates (ls^{-1}) for the calibration periods E4, SA1 and WS1 for which no filling of missing observations was performed and hence the peak flow observations are probably missing are respectively 130.3, 140.1, 432.3. The peakiest

flow rate for the WS1 indicate that snowmelt or rainfall on snowmelt induced urban runoff during the winter-spring (WS) seasons may result in the peakiest flow rates in the catchment that could be important for reliable determination of the capacity of sewer pipes. Therefore, determination of design floods by including simulation of urban floods during snow-influenced seasons would be required for cold climate regions as suggested by Watt and Marsalek (2013). Hence, improved simulation of snowmelt-influenced runoff through comparative evaluation of the performances of the simple to more complex (e.g. energy balance) urban snow models would be necessary. The slight underestimation of peak flows in the present study may also be related to spatial variability of precipitation within the catchment that could not be captured by the single climate station located near the outlet of the catchment. The spatially distributed modelling of the present study was utilized mainly for representation of the the spatial distribution of imperviousness (e.g. see Mejía and Moglen, 2010) or for classification of the land use (land cover) in the catchment in to roofs (buildings), paved roads, built-up areas and open areas, and then to model the hydrological processes accordingly. However, precipitation records from the single station should be reasonably sufficient for the small size (21.255ha) catchment based on recommendations from previous studies (e.g., Schilling, 1991; Berne et al., 2004; Bruni et al. 2015; Ochoa-Rodriguez et al., 2015). Nevertheless, parameter calibration and investigation of the urban hydrological processes using dense precipitation gauges would be important for better representation of the spatial variability of precipitation.

In the present study, there is no saturation excess surface runoff, which agrees with previous studies that neglect this runoff generating mechanism in urban catchments (e.g. Rodriguez et al., 2008, Coutu et al., 2012). The catchment soil moisture state never reached the full saturation level (i.e. $SS < SS_{max}$) during the calibration periods. Therefore, the infiltration process from the previous surfaces was found to be governed by the infiltration capacity of the surfaces and not by the soil moisture state from below. However, the infiltration modelling used in the present study is based on parametrizing by the infiltration capacity parameters for pervious

surfaces and hence dominant influence of the infiltration capacity of the surface is expected. The infiltrated water volume resulting in the $Q_{Tsubsurface}$ ($Q_{Tsubsurface}/P = 60.38\% - 78.83\%$) agrees with Rodriguez et al. (2008) who found that the I/P of 60.1% for natural surfaces and 71.7% for the total catchment by allowing infiltration on roofs and street surfaces. In the present study, the interaction between the groundwater flow and the sewer pipes was found to be negligible due to the negligible percolation, even if the percolation was computed before computation of the interflow from soil moisture storage. The P-R model in the present study is not capable of simulating the groundwater levels. Moreover, it is not easy to know the exact locations of the two-way interactions between the subsurface runoff and cracked sewer pipes. Therefore, the subsurface model structure of the present study can be simplified to a single subsurface storage and subsurface runoff component interacting with the flow in the sewer pipes that would also allow reducing the number of calibrated parameters in the runoff response routine.

In the present study, the total evapotranspiration is dominated by actual evaporation from surface depression storage (AE) rather than the evapotranspiration from the soil moisture (AET), which does not agree with Rodriguez et al. (2008) who found that there is marked transpiration (T) from the vadose zone from natural surfaces ($T/P = 43.5\%$) while the surface evaporation is relatively low. The difference occurred due to the low evapotranspiration from the soil moisture storage for the cold climate region of the present study and probably due to the conceptualization that the total generated subsurface runoff contribute to flow in the sewer pipes in Rodriguez et al. (2008) and hence the calibration had to overestimate the transpiration loss from the vadose zone to provide better performance measure. The present study indicated that there is a marked total evapotranspiration loss only for the warm seasons calibration (i.e. $ET/P = 18.18\%$ for SA1), which agrees with Ragab et al. (2003) who found that 21–24% of annual rainfall evaporates and Ramier et al. (2011) who found that evaporation losses represent 20% of the total rainfall. The present study indicated that the effects of surface depression

storage on generated runoff volume is high for the event-based calibration than the long-term (seasonal) calibrations while the effect of surface water storage in terms of the snow water equivalent (SWE) is obviously high for the snow-influenced seasons.

Runoff routing

For runoff routing, the flow travel length estimated for the sub-catchments were used for all grid cells in the sub-catchments assuming the same entry time to the conduits for all grid cells within each sub-catchment. In addition, an effective (calibrated) shape factor (*SF*) parameter was used for all sub-catchments and hence the flow travel length outside the pipes for the sub-catchments are dependent only on the areas of the sub-catchments. Despite these simplifications, the flow path response function based on an analytical solution to the diffusion wave equation and the source-to-sink (STS) used in the present study was found to provide an acceptable runoff delay in the stormwater network, which agrees with Mays (2001) and Borah (2011) who suggested the diffusion wave equation and its analytical solutions as a balance between complexity and accuracy, and Mejia and Moglen (2010) and Cantone and Schmidt (2011) who reported good performances of the runoff routing algorithm for urban catchments. However, the calibration resulted in different values of the runoff routing parameters for the calibration periods, which resulted in different mean flow travel times, Peclet numbers, and hence the STS response functions for the sub-catchments among the calibration periods. This may affect the validation (transferability of calibrated parameters of the routing model among the calibration periods), which may require investigation of the effects on the validation of the transferability of runoff generation and runoff routing parameters separately.

Conclusions

The present study presented a spatially distributed (5mx5m grids) Precipitation-Runoff modelling at a temporal resolution of 2min for a small (21.255ha) separate stormwater drainage catchment located in cold climate and hence influenced by snow seasonality. Parameter calibration and validation based on events and seasons were conducted using the hydro-

climatic records of the Risvollan stormwater catchment in Trondheim City (Norway). The study involved modelling of the dominant components of the urban precipitation water cycle including surface depression storage, snow accumulation and melt processes, infiltration excess and saturation excess surface runoff, infiltration, subsurface runoff from soil moisture and groundwater storages, contributions of the subsurface runoff to the flow in the sewer drainage system, evapotranspiration from depression and soil moisture storages and percolation to groundwater, and runoff routing.

By modelling the interaction between the surface depression and soil storages with the atmosphere in terms of evapotranspiration flux, the model indicated that the impact of surface depression storage on the simulated runoff volume in the sewer pipes is high for event-based simulation while the impact of evapotranspiration is high only for the long-term (seasonal) simulation during warmer (Summer-Autumn) seasons. Including the subsurface components of the urban precipitation water budget allows estimating the proportion of infiltrated water contributing to the generation of subsurface runoff. In addition, parameterization of a two-way interaction between the subsurface runoff and the flow in the sewer pipes based on setting the percentages of subsurface runoff contributing to the flow in sewer pipes as effective (calibrated) parameters applied to all grids allows estimation of subsurface runoff contribution to the flow in the artificial sewer drainage system. As investigated in the present study, the contributions of the subsurface runoff to the flow in the sewer pipes may be higher than the contribution of surface runoff and hence runoff simulation for estimation of floods for design and management of water infrastructure should consider the subsurface runoff components of the urban precipitation water cycle. The study for the snow-influenced (Winter-Spring) periods indicated that the peakiest flow rate in cold climates may be associated to the snowmelt or rainfall on snowmelt events and hence estimation of urban floods should include simulation of urban runoff during snow-influenced seasons.

Despite the several simplifying assumptions in the analytical solution of the diffusion wave equation flow path response function based source-to-sink (STS) routing used in the present study, the routing algorithm is able to provide acceptable runoff delay and attenuation of peaks in the stormwater network.

The spatial distributed model is useful for better representation of the spatial distribution of precipitation and land use (land cover) in the catchment for better simulation of runoff response and hence estimation of design flood, for evaluation of performances of different stormwater management techniques, for assessment of the impacts of land use and climate change, etc.

In spite of the fact that the contribution of the present study was geared towards the spatially distributed P-R modelling of the dominant components of the urban precipitation water cycle including the evapotranspiration, snow and subsurface processes, there are several urban hydrological-hydraulic conditions and uncertainties associated to the P-R modelling that need further investigation contingent on further data availability or data acquisition: (i) the effects of feedback mechanisms between all aspects of urban water cycle including leakages from water supply systems and faulty or illegal connections between the wastewater and stormwater systems (e.g. see Fletcher et al., 2013); (ii) the parameterization for a two-way interaction between the subsurface runoff and sewer pipes of the present study do not involve information on the elevations of the sewer pipes and groundwater level, and actual locations of the interactions (i.e. cracked sewer pipes or joints) while the latter is practically not easy to identify in a field, for instance, Karpf and Krebs (2011) related the CCTV-data based pipe age classes to groundwater infiltration to sewer pipes; (iii) there are large numbers of calibrated parameters in the present study since parameter uncertainty and identifiability analyses were not objectives of the present study and hence efforts for model parsimony by reducing the numbers of calibrated parameters based on parameter sensitivity analyses and assessment of parameter uncertainty are important; and (iv) the routing algorithm of the present study does not involve detailed analyses of sewer hydraulics and hence coupling of the spatially distributed runoff

generation model to the existing sewer hydraulics models like the SWMM runoff routing engine (Huber and Dickinson, 1988; Rossman, 2004) may be important for detailed hydraulic studies like sewer surcharge, combined sewer overflows, surface inundation due to urban flooding, etc.

Acknowledgments

We found the observed flow data at the outlet of the Risvollan stormwater catchment from the Norwegian Water resources and Energy directorate (NVE) database. We are thankful to Mr. Carlos Monrabal-Martinez of the department of Civil and Environmental Engineering (NTNU) for providing us the climate data of the Risvollan catchment used in the present study. The Norwegian University of Science and Technology (Trondheim) funded the research.

References

- Allen, R.G., Pereira, L.S., Raes, D. & Smith, M. 1998 Crop evapotranspiration: guidelines for computing crop water requirements. Irrigation and Drainage Paper No. 56, Food and Agriculture Organization of the United Nations, Rome, Italy.
- Baker, D. G., Ruschy, D. L., and Wall, D. B.: The albedo decay of prairie snows, *J. Appl. Meteor.*, 29, 179–187, 1990.
- Balascio, C. C., D. J. Palmeri, and H. Gao (1998), Use of a genetic algorithm and multi-objective programming for calibration of a hydrologic model, *Trans. ASAE*, 41, 615– 619.
- Barnard, T., A. Kuch, G.R. Thompson, S. Mudaliar and B.C. Phillips. 2007. "Evolution of an Integrated 1D/2D Modeling Package for Urban Drainage." *Journal of Water Management Modeling* R227-18. doi:10.14796/JWMM.R227-18.

- Barron, O.V., Barr, A.D., Donn M.J. 2013. Effect of urbanisation on the water balance of a catchment with shallow groundwater. *Journal of Hydrology* 485, 162–176.
- Bengtsson, L., Semádeni-Davies A., 2011. Urban snow. In Vijay P. Singh, Pratap Singh & Umesh K. Haritashya (eds.), *Encyclopedia of Snow, Ice and Glaciers*, DOI 10.1007/978-90-481-2642-2, Springer Science+Business Media B.V.
- Berg, A. A., and Byrne, J. M. (1998). Water table development due to household and park irrigation in Lethbridge, Alberta. *Can. Water Resour. J.*, Cambridge, Ontario, 23(1), 61–75.
- Bergström, S. 1976 Development and application of a conceptual runoff model for Scandinavian catchments, *SMHI Reports RHO*, No. 7, Norrköping.
- Berne, A., Delrieu, G., Creutin, J-D., Oble C. 2004. Temporal and spatial resolution of rainfall measurements required for urban hydrology. *Journal of Hydrology* 299, 166–179.
- Berthier E, Andrieu H, Creutin JD. 2004. The role of soil in the generation of urban runoff: development and evaluation of a 2D model. *J Hydrol* 299:252–66.
- Bicknell, B.R., Imhoff, J.C., Kittle Jr, J.L., Jobes, T.H., Donigian Jr, A.S., and Johanson, R., 2001. *Hydrological Simulation Program–FORTRAN: HSPF Version 12 User’s Manual*. Mountain View, CA: AQUA TERRA Consultants.
- Borah, D.K. 2011. Hydrologic procedures of storm event watershed models: a comprehensive review and comparison. *Hydrol. Process.* 25, 3472–3489.
- Braud, I., Breil, P., Thollet, F., Lagouy, M., Branger, F., Jacqueminet, C., Kermadi, S., Michel, K. 2013. Evidence of the impact of urbanization on the hydrological regime of a medium-sized periurban catchment in France. *Journal of Hydrology* 485, 5–23.
- Brooks, E. S., J. Boll, and P. A. McDaniel (2007), Distributed and integrated response of a geographic information system based hydrologic model in the eastern Palouse region, Idaho, *Hydrol. Processes*, 21, 110– 122.

- Bruni, G. Reinoso, R., van de Giesen, N. C., Clemens, F. H. L. R., ten Veldhuis, J. A. E. 2015. On the sensitivity of urban hydrodynamic modelling to rainfall spatial and temporal resolution. *Hydrol. Earth Syst. Sci.*, 19, 691–709.
- Burns, D., Vitvar, T., McDonnell, J., Hassett, J., Duncan, J., Kendall, C., 2005. Effects of Suburban development on runoff generation in the Croton River basin, New York, USA. *Journal of Hydrology*, 311(1-4), 266-281.
- Camici, S., Tarpanelli, A., Brocca, L., Melone, F., Moramarco, T. 2011. Design soil moisture estimation by comparing continuous and storm-based rainfall-runoff modeling. *WATER RESOURCES RESEARCH*, VOL. 47, W05527, doi:10.1029/2010WR009298.
- Cantone, J., Schmidt A. 2011. Dispersion mechanisms and the effect of parameter uncertainty on hydrologic response in urban catchments. *WATER RESOURCES RESEARCH*, VOL. 47. W05503, doi:10.1029/2010WR009331.
- Cheng S-j, Wang R-y. 2002. An approach for evaluating the hydrological effects of urbanization and its application. *Hydrological Processes* 16:1403–1418. DOI: 10.1002/hyp.350.
- Coutu, S., Giudice, DD., Rossi, L., Barry DA. 2012. Parsimonious hydrological modeling of urban sewer and river catchments. *Journal of Hydrology* 464–465, 477–484.
- Cuo, L., Lettenmaier, D.P., Mattheussen, B.V., Storck, P., Wiley M. 2008. Hydrologic prediction for urban watersheds with the Distributed Hydrology–Soil–Vegetation Model. *Hydrol. Process.* 22, 4205–4213.
- DeFries, R., Eshleman, N.K., 2004. Land-use change and hydrologic processes: a major focus of the future. *Hydrol. Process.* 18 (11), 2183–2186.
- Delleur, J.W., 2003. The evolution of urban hydrology: past, present, future. *J. Hydraul. Eng.* ASCE 129 (8), 563–573.

- Denault C, Millar RG, Lence BJ. 2006. Assessment of possible impacts of climate change in an urban catchment. *JAWRA Journal of the American Water Resources Association* 42: 685–697. DOI: 10.1111/j.1752-1688.2006.tb04485.x.
- Dietz ME, Clausen JC. 2008. Stormwater runoff and export changes with development in a traditional and low impact subdivision. *Journal of Environmental Management* 87: 560–566. DOI: 10.1016/j.jenvman.2007.03.026.
- Dirckx, G., Bixio, D., Thoeye, C., De Gueldre, G., Van De Steene, B., 2009. Dilution of sewage in Flanders mapped with mathematical and tracer methods. *Urban Water J.* 6 (2), 81–92.
- Domingo, N.D. Sto., Refsgaard, A., Mark, O., Paludan, B. 2010. Flood analysis in mixed-urban areas reflecting interactions with the complete water cycle through coupled hydrologic-hydraulic modelling. *Water Science and Technology* 62 (6).
- Du, J., Xie, H., Hua, Y., Xu, Y., Xu, Chong-Yu. 2009. Development and testing of a new storm runoff routing approach based on time variant spatially distributed travel time method. *Journal of Hydrology* 369, 44–54.
- Easton, Z.M., Ge´rard-Marchant, P., Walter, M.T., Petrovic, A.M., Steenhuis, TS. 2007. Hydrologic assessment of an urban variable source watershed in the northeast United States. *WATER RESOURCES RESEARCH*, VOL. 43, W03413, doi:10.1029/2006WR005076.
- Elga, S., Jan, B., Okke B. 2015. Hydrological modelling of urbanized catchments: A review and future directions. *Journal of Hydrology* 529: 62–81.
- Elliott, A.H., Trowsdale, S.A., 2007. A review of models for low impact urban stormwater drainage. *Environ Modell. Software* 22, 394–405.
- Fassman-Beck, E., Voyde, E., Simcock, R., Hong, Y.S., 2013. 4 Living roofs in 3 locations: does configuration affect runoff mitigation? *J. Hydrol.* 490, 11–20.

- Fletcher, T.D., Andrieu, H., Hamel, P. 2013. Understanding, management and modelling of urban hydrology and its consequences for receiving waters: A state of the art. *Advances in Water Resources* 51, 261–279.
- Freni, G., Mannina, G., Viviani, G., 2010. Urban storm-water quality management: centralized versus source control. *J. Water Resour. Plan. Manage.* 136 (2), 268–278.
- Grayson, R., I. D. Moore, and T. A. McMahon (1992), Physically based hydrologic modeling: 2. Is the concept realistic, *Water Resour. Res.*, 28, 2659– 2666.
- Gallo, K., Hale, R., Tarpley, D., Yu, Y. 2011. Evaluation of the Relationship between Air and Land Surface Temperature under Clear- and Cloudy-Sky Conditions. *JOURNAL OF APPLIED METEOROLOGY AND CLIMATOLOGY* 50, 767-775.
- Gironás, J., Niemann, J.D., Roesner, L.A. Rodriguez, F., Andrieu H. 2009. A morpho-climatic instantaneous unit hydrograph model for urban catchments based on the kinematic wave approximation. *Journal of Hydrology* 377 (3–4), 317–334
- Green, W. H. and G. Ampt. 1911. Studies of Soil Physics, Part 1. The flow of air and water through soils. *Journal of Agricultural Science* 4: 1-24.
- Grimmond, C.S.B., Oke, T.R., 1991. An evapotranspiration-interception model for urban areas. *Water Resour. Res.* 27 (7), 1739–1755.
- Grimmond, C.S.B. et al. 2009. Urban Surface Energy Balance Models: Model Characteristics and Methodology for a Comparison Study. In Baklanov, A. et al. (eds.), *Meteorological and Air Quality Models for Urban Areas*, DOI 10.1007/978-3-642-00298-4_11, Springer-Verlag Berlin Heidelberg.
- Guan M, Sillanpää N, Koivusalo H. 2015. Modelling and assessment of hydrological changes in a developing urban catchment. *Hydrol. Process.* 29, 2880–2894.
- Guan, M., Sillanpää, N., Koivusalo, H. 2016. Storm runoff response to rainfall pattern, magnitude and urbanization in a developing urban catchment. *Hydrol. Process.* 30, 543–557.

Guo, JCY, Urbonas B., 2009. Conversion of Natural Watershed to Kinematic Wave Cascading Plane. *J. Hydrol. Eng.*, 2009, 14(8): 839-846.

Haase, D. 2009. Effects of urbanisation on the water balance – A long-term trajectory. *Environmental Impact Assessment Review* 29, 211–219.

Hailegeorgis, TT, Alfredsen, K., 2017. Analyses of extreme precipitation and runoff events including uncertainties and reliability in design and management of urban water infrastructure. *Journal of Hydrology* 544 290–305.

Hailegeorgis, TT, Alfredsen, K., Abdella, YS, Kolberg, S. 2015. Evaluation of different parameterizations of the spatial heterogeneity of subsurface storage capacity for hourly runoff simulation in boreal mountainous watershed. *Journal of Hydrology* vol. 522, 522–533.

Hamel, P. Edoardo D., Fletcher TD. 2013. Source-control stormwater management for mitigating the impacts of urbanisation on baseflow: A review. *Journal of Hydrology* 485, 201–211.

Hayami, S., 1951. On the propagation of flood waves. *Disaster Prev. Res. Inst. Bull.* 1, 1–16.

Hegdahl, T.J., Tallaksen, L.M., Engeland, K., Burkhart J.F., Xu C-Y. 2016. Discharge sensitivity to snowmelt parameterization: a case study for Upper Beas basin in Himachal Pradesh, India. *Hydrology Research* 47 (4).

Herb WR, Janke B, Mohseni O, Stefan HG. 2009. Runoff Temperature Model for Paved Surfaces. *J. Hydrol. Eng.* 14(10): 1146–1155.

Horton, R.E., 1940. An approach towards a physical interpretation of infiltration capacity. *Soil Sci. Soc. Am. Proc.* 5, 399–417.

Huber, W., Dickinson, R.E., 1988. Storm Water Management Model, Version 4: User's Manual. U.S. EPA, Athens, Georgia. EPA/600/3e88/001a.

Jacobson, C. R. 2011. Identification and quantification of the hydrological impacts of imperviousness in urban catchments: A review. *Journal of Environmental Management* 92, 1438–1448.

- Joss A., Siegrist H, Ternes TA. Are we about to upgrade wastewater treatment for removing organic micropollutants?. *Water Sci Technol.* 2008;57(2):251-5. doi: 10.2166/wst.2008.825.
- Karpf, C., Krebs P. 2011. Quantification of groundwater infiltration and surface water inflows in urban sewer networks based on a multiple model approach. *water research* 45, 3129-3136.
- Koutsoyiannis D. 2012. Clausius–Clapeyron equation and saturation vapour pressure: simple theory reconciled with practice. *Eur. J. Phys.* 33 (2012) 295–305 doi:10.1088/0143-0807/33/2/295.
- Krebs G, Kokkonen T, Valtanen M, Setälä H, Koivusalo H. 2014. Spatial resolution considerations for urban hydrological modelling. *Journal of Hydrology* 512: 482–497. DOI: 10.1016/j.jhydrol.2014.03.013.
- Lee, A., Hewa, G., Pezzaniti, D., Argue, J.R., 2008. Improving stream low flow regimes in urbanised catchments using water sensitive urban design techniques. *Aust. J. Water Resour.* 5, 121–132.
- Lhomme, J., Bouvier, C., Perrin, J.L., 2004. Applying a GIS-based geomorphological routing model in urban catchments. *Journal of Hydrology* 299 (3–4), 203–216.
- Marsalek, J., Jiménez-Cisneros, B., Karamouz, M., Malmquist, P.-A., Goldenfum, J., Chocat, B., 2007. *Urban Water Cycle Processes and Interactions: Urban Water Series – UNESCO-IHP.* Springer, Berlin.
- Mathuesen, B.V., 2004. *Effects of Anthropogenic Activities on Snow Distribution, and Melt in an Urban Environment.* Norwegian University of Science and Technology, PhD. Dissertation. Faculty of Engineering Science and Technology.
- Mays, L.W., *Stormwater collection systems handbook,* McGraw-Hill, Quebecor/Martinsburg, USA, 2001.
- Mejía A.I., Moglen, G.E. 2010. Impact of the spatial distribution of imperviousness on the hydrologic response of an urbanizing basin. *Hydrol. Process.* 24, 3359–3373.

- Miller, J.D., Kim, H., Kjeldsen, T.R., Packman, J., Grebby, S., Dearden, R. 2014. Assessing the impact of urbanization on storm runoff in a peri-urban catchment using historical change in impervious cover. *Journal of Hydrology* 515, 59–70.
- Moghadas S., Gustafsson, A-M, Muthanna, T.M., Marsalek, J., Viklander M. 2015. Review of models and procedures for modelling urban snowmelt. *Urban Water Journal*, DOI: 10.1080/1573062X.2014.993996.
- Nauman, E.B., 1981. Residence time distributions in systems governed by the dispersion equation. *Chem. Eng. Sci.* 36, 957–966.
- Nash, J.E., Sutcliffe, J.V., 1970. River flow forecasting through conceptual models. Part I – A discussion of principles. *J. Hydrol.* 10, 282–290.
- Ochoa-Rodriguez, S., Wang, L.-P., Gires, A., Rui Pina, D., Reinoso-Rondinel, R., Bruni, G., Ichiba, A., Gaitan, S., Cristiano, E., van Assel, J., Kroll, S., Murlà-Tuyls, D., Tisseran, B., Schertzer, D., Tchiguirinskaia, I., Onof, C., Willems, P., ten Veldhuis, M.-C. 2015. Impact of spatial and temporal resolution of rainfall inputs on urban hydrodynamic modelling outputs: A multi-catchment investigation. *Journal of Hydrology* 531: 389–407.
- Olivera, F., Maidment, D.R., 1999. Geographic information system (GIS)-based spatially distributed model for runoff routing. *Water Resour. Res.* 35 (4), 1155–1164.
- Owens, P.N., Walling, D.E., 2002. The phosphorus content of fluvial sediment in rural and industrialized river basins. *Water Research* 36, 685e701.
- Pan, A., Hou, A., Tian, F., Ni, G., Hu, H., 2012. Hydrologically enhanced distributed urban drainage model and its application in Beijing city. *J. Hydrol. Eng.* 17 (6), 667–678.
- Paz, A. R., Meller, A., Silva G. B. L. 2011. Coupled 1D-2D hydraulic simulation of urban drainage systems: model development and preliminary results. 12nd International Conference on Urban Drainage, Porto Alegre/Brazil, 11-16 September 2011.
- Petrucci, G., Bonhomme C. 2014. The dilemma of spatial representation for urban hydrology

semi-distributed modelling: Trade-offs among complexity, calibration and geographical data. *Journal of Hydrology* 517, 997–1007.

Philip, J. R. 1957. The theory of infiltration: 1. The infiltration equation and its solution. *Soil Sci.* 83, 345–357.

Priestley, C.H.B., Taylor, R.J., 1972. On the assessment of surface heat flux and evaporation using large-scale parameters. *Mon. Weather Rev.* 100, 81–82.

Raleigh, M.S. Landry, C.C. Hayashi, M., Quinton, W.L., Lundquist, J.D. 2013. Approximating snow surface temperature from standard temperature and humidity data: New possibilities for snow model and remote sensing evaluation *WATER RESOURCES RESEARCH*, VOL. 49, 8053–8069, doi:10.1002/2013WR013958.

Ragab R, Rosier P, Dixon A, Bromley J, Cooper JD. 2003. Experimental study of water fluxes in a residential area: 2. Road infiltration, runoff and evaporation. *Hydrol Process* 17:2423–37.

Ramier D, Berthier E, Andrieu H. 2011. The hydrological behaviour of urban streets: long-term observations and modelling of runoff losses and rainfall, runoff transformation. *Hydrol Process* 25:2161–78.

Rodriguez, F., Andrieu, H., Zech, Y., 2000. Evaluation of a distributed model for urban catchments using a 7-year continuous data series. *Hydrological Processes* 14 (5), 899–914.

Rodriguez, F., Andrieu, H., Creutin, J.D., 2003. Surface runoff in urban catchments: morphological identification of unit hydrographs from urban databanks. *Journal of Hydrology* 283 (1–4), 146–168.

Rodriguez, F., Cudennec, C., Andrieu, H., 2005a. Application of morphological approaches to determine unit hydrographs of urban catchments. *Hydrological Processes* 19 (5), 1021–1035.

Rodriguez, F., Morena, F., Andrieu, H., 2005b. Development of a distributed hydrological model based on urban databanks-production process of URBS. *Water Science and Technology* 52(5), 241-248.

- Rodriguez, F., Andrieu, H., Morena, F. 2008. A distributed hydrological model for urbanized areas – Model development and application to case studies. *Journal of Hydrology* 351, 268–287.
- Rossman, L.A., 2004. Storm Water Management Model. Version 5.0. National Risk Management Research Laboratory, United States Environmental Protection Agency, Cincinnati, Ohio.
- Rossman, L.A., Dickinson, R.E., Schade, T., Chan, C., Burgess, E.H. and Huber, W.C. (2005). SWMM 5: The USEPA's newest tool for urban drainage analysis. 10th International Conference on Urban Drainage, Copenhagen/Denmark, 21-26 August 2005.
- Rutter, A.J., Kershaw, K.A., Robins, P.C., Morton, A.J., 1971. A predictive model of rainfall interception in forests: 1-Derivation of the model from observations in a plantation of Corsican pine. *Agricultural Meteorology* 9, 367–384.
- Schilling, W. 1991. Rainfall data for urban hydrology: what do we need?. *Atmospheric Research*, 27, 5-21.
- Seibert, J., 2002. HBV light–User's manual. Uppsala, Sweden: Department of Earth Sciences and Hydrology, Uppsala University.
- Shuster WD, Bonta J, Thurston H, Warnemuende E, Smith DR. 2005. Impacts of impervious surface on watershed hydrology: a review. *Urban Water Journal* 2: 263–275. DOI: 10.1080/15730620500386529.
- Sicart, J.E., Pomeroy, J.W., Essery, R.L.H., Bewley, D., 2006. Incoming longwave radiation to melting snow: observations, sensitivity and estimation in northern environments. *Hydrol. Process.* 20, 3697–3708.
- Singh, V.P., Aravamuthan, V., 1996. Errors of kinematic–wave and diffusion–wave approximations for steady-state overland flows. *Catena* 27, 209–227.

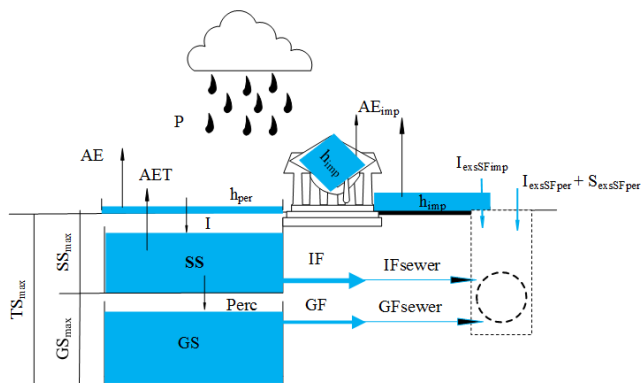
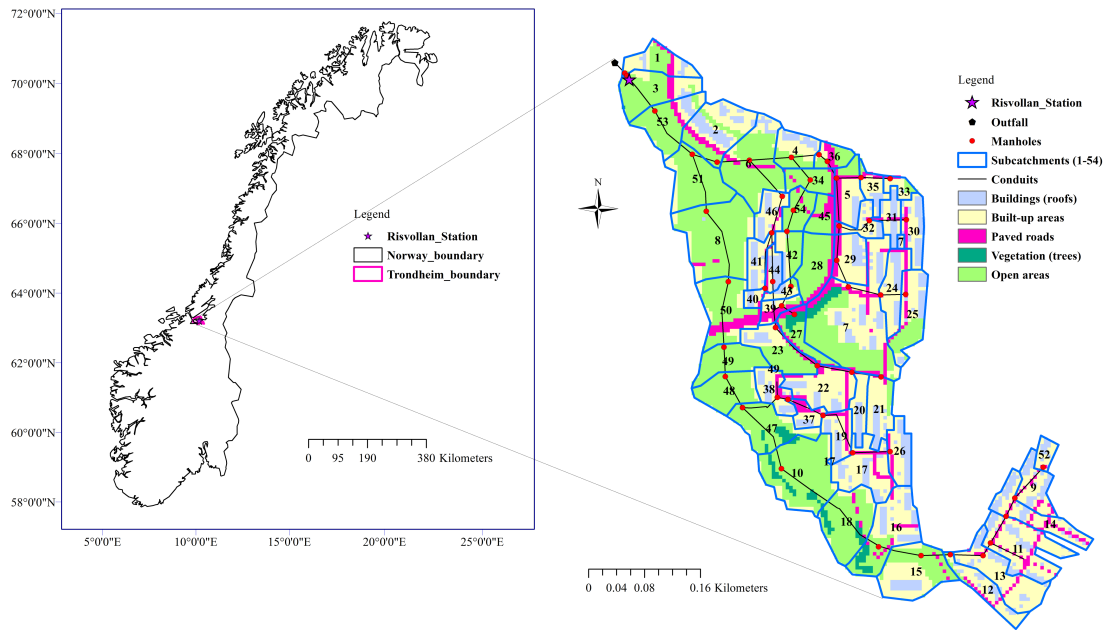
- Stewart, R D., Rupp, D.E., Abou Najm, M. R., Selker, J. S. 2013. Modeling effect of initial soil moisture on sorptivity and infiltration. *WATER RESOURCES RESEARCH*, VOL. 49, 7037–7047, doi:10.1002/wrcr.20508.
- Tarboton, David G., Chowdhury, Tanveer G., Jackson, Thomas H. 1994. A Spatially Distributed Energy Balance Snowmelt Model. Reports. Paper 60, Utah Water Research Laboratory http://digitalcommons.usu.edu/water_rep/60. Accessed on 03.04.2017.
- Thorndahl, S., Einfalt, T., Willems, P., Nielsen, J.E., ten Veldhuis, M-C, Arnbjerg-Nielsen, K., Rasmussen, M.R., Molnar, P. 2017. Weather radar rainfall data in urban hydrology. *Hydrol. Earth Syst. Sci.*, 21, 1359–1380.
- Tøfte, LS, Kolberg S. 2016. ENKI-rutine: HBVSnow. SINTEF Energi AS, Trondheim.
- United Nations. World urbanization prospects: the 2009 revision. New York: United Nations Department of Economic and Social Affairs (Population Division); 2010.
- Valeo, C., Ho, C.L.I. 2004. Modelling urban snowmelt runoff. *Journal of Hydrology* (299), 237–251.
- Valtanen M, Sillanpää N, Setälä H. 2014. Effects of land use intensity on stormwater runoff and its temporal occurrence in cold climates. *Hydrological Processes* 28: 2639–2650. DOI: 10.1002/hyp.9819.
- van Genuchten M. T. 1980 A closed-form equation for predicting the hydraulic conductivity of unsaturated soils. *Soil Science Society of America Journal* 44, 892–898.
- Verseghy, D. L.: CLASS – A Canadian land surface scheme for GCMS. 1, *Soil Model, Int. J. Clim.*, 11, 111–133, 1991.
- Walsh CJ, Roy AH, Feminella JW, Cottingham PD, Groffman PM, Morgan RP. The urban stream syndrome: current knowledge and the search for a cure. *J N Am Benthol Soc* 2005; 24:706–23.
- Watt, E., Marsalek, J., 2013. Critical review of the evolution of the design storm event concept. *Can. J. Civ. Eng.* 40, 105–113.

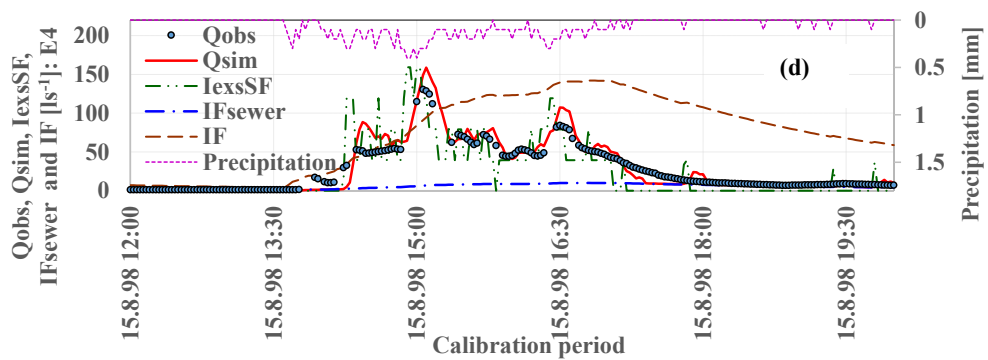
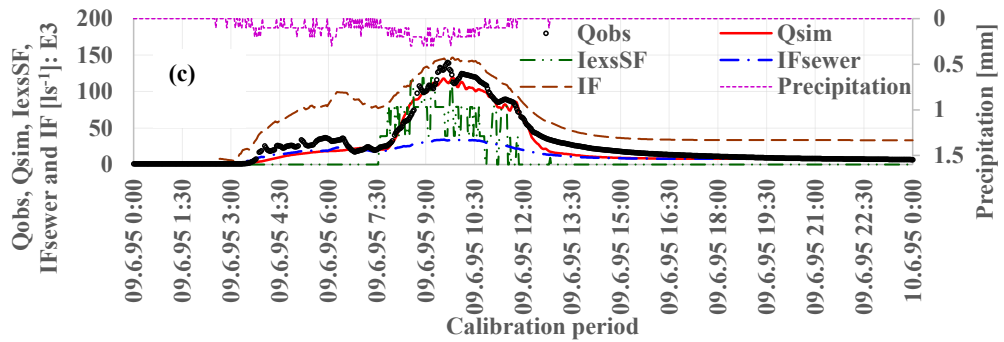
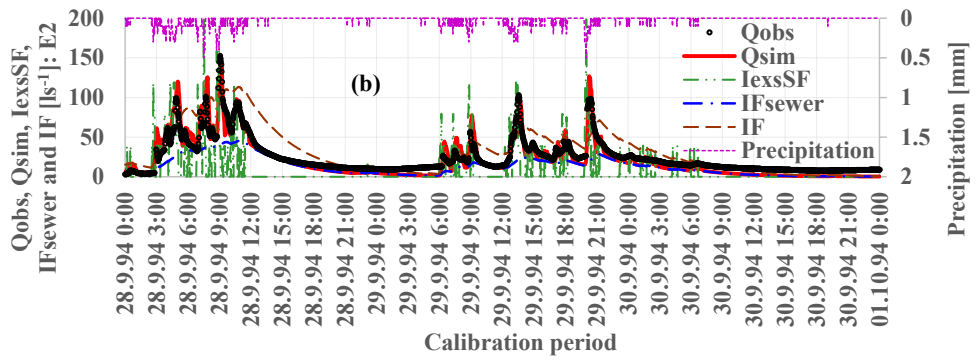
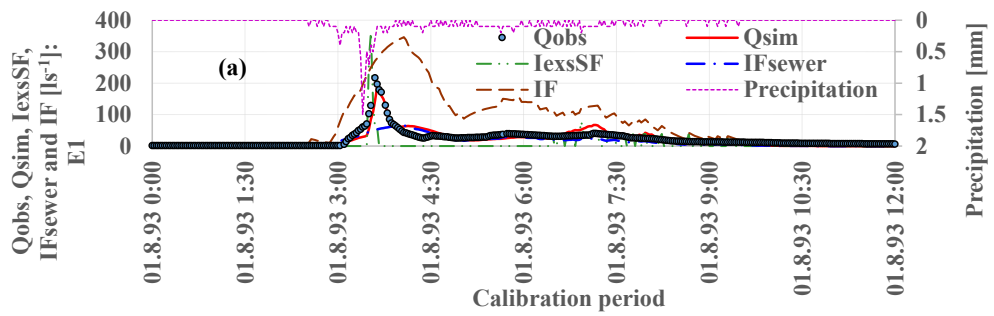
Wei, G., Brombach, H., Haller, B., 2002. Infiltration and inflow in combined sewer systems: long-term analysis. *Water Sci. Technol.* 45 (7), 11–19.

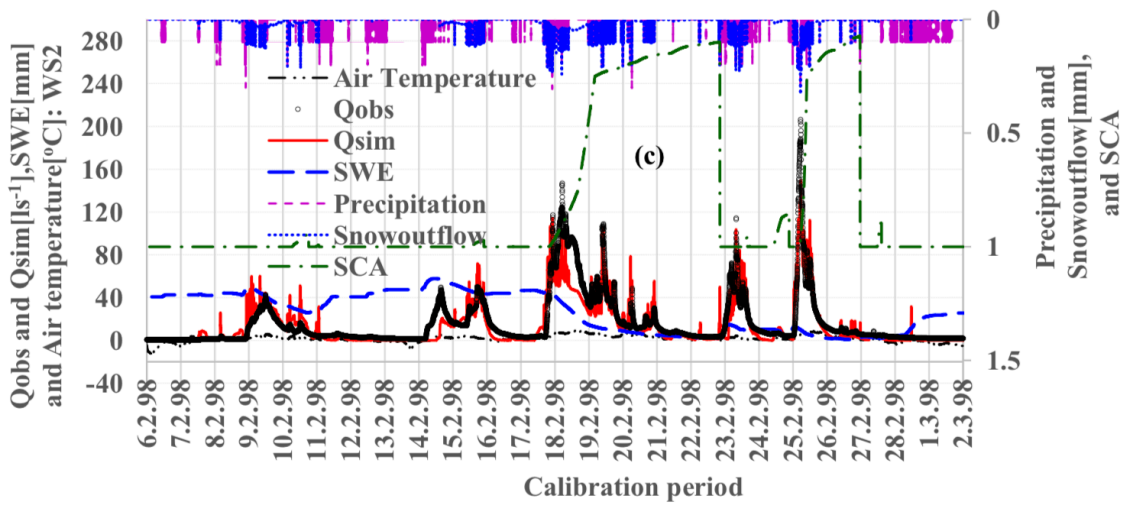
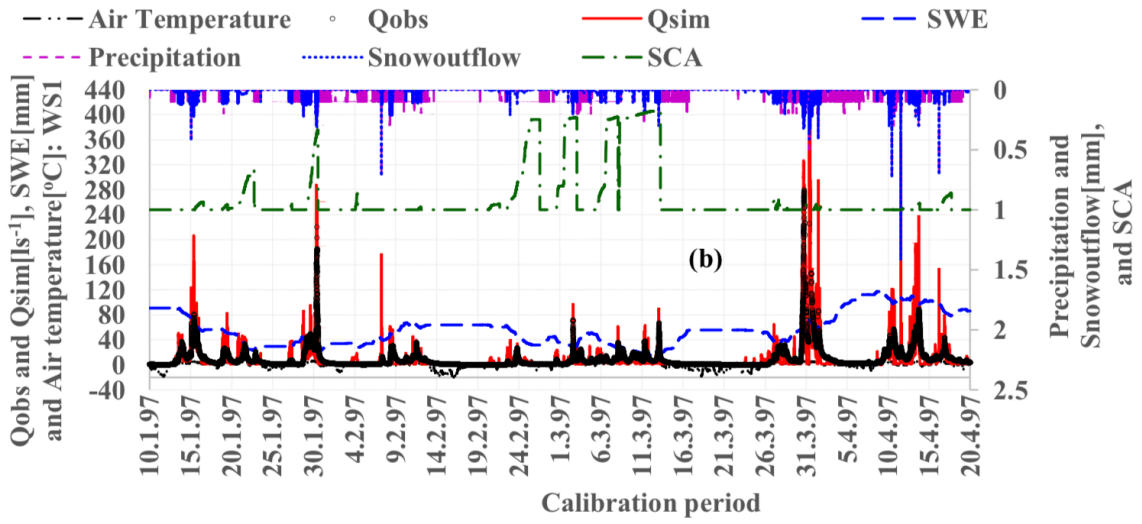
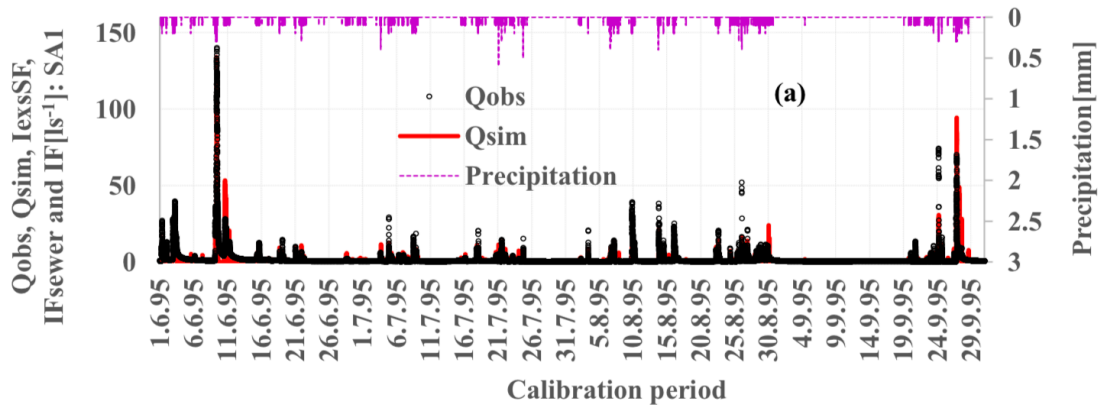
Xiong, Yiyi, Melching, CS. 2005. Comparison of Kinematic-Wave and Nonlinear Reservoir Routing of Urban Watershed Runoff. *J. Hydrol. Eng.*, 2005, 10(1): 39-49.

Zhu, Z., Oberg, N., Morales, V.M., Quijano, J.C., Landry, B.J., Garcia, M.H. 2016. Integrated urban hydrologic and hydraulic modelling in Chicago, Illinois. *Environmental Modelling & Software* 77, 63-70.

Zoppou, C. 2001. Review of urban storm water models. *Environmental Modelling & Software* 16 195–231.







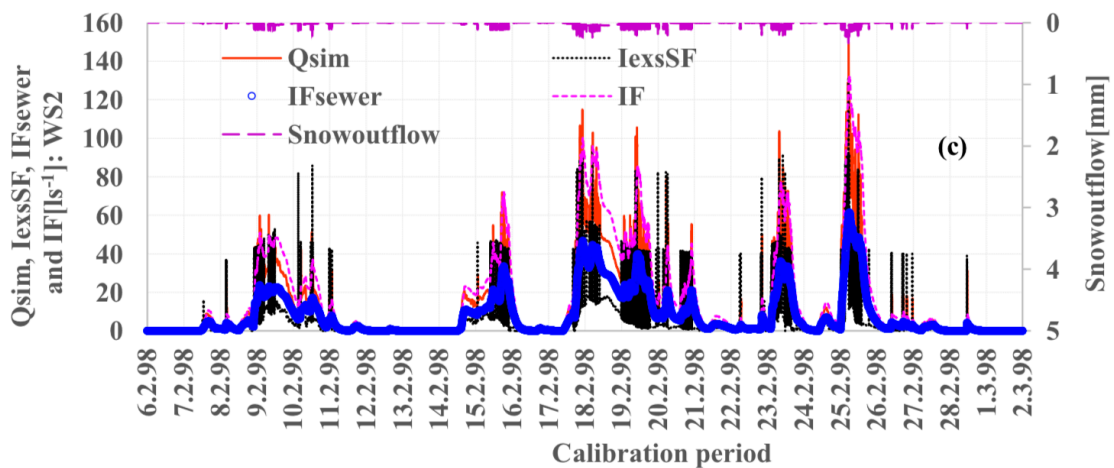
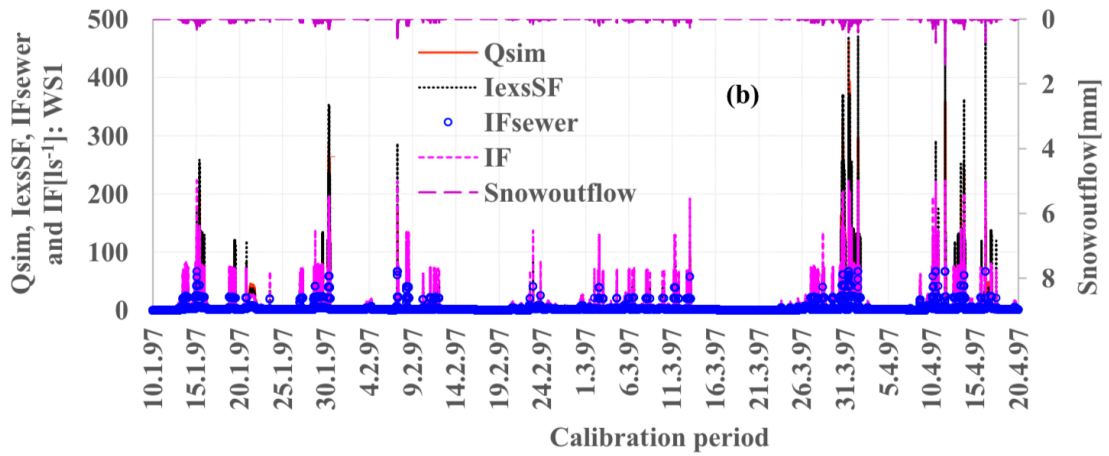
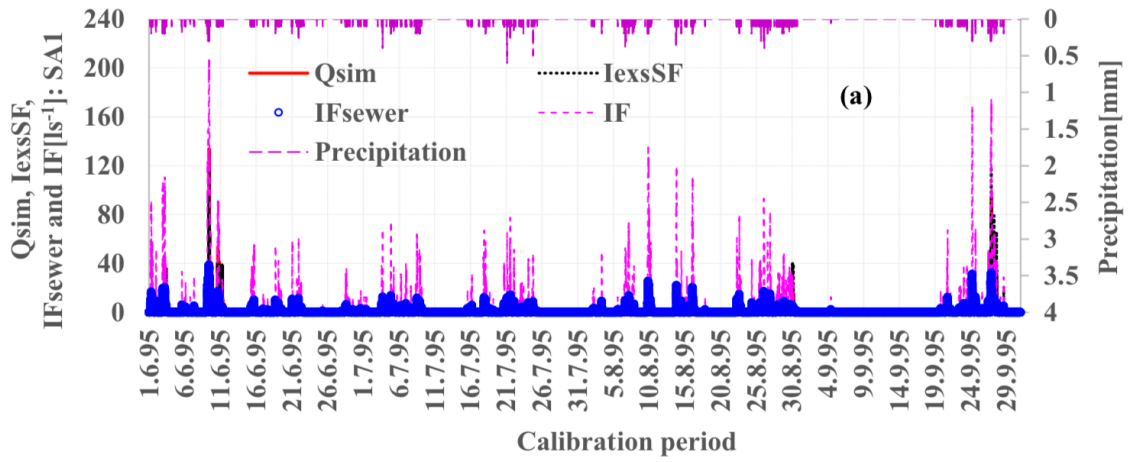


Table 1. Calibrated parameters and their minimum (Min.) and maximum (Max.) values.

Calibrated parameters	Unit	Model	Parameter ranges		Description
			Min.	Max.	
c1	-	PET	-1.00	0.50	Intercept for T _{sn} and T _a linear regression
c1L	-	PET	-1.00	1.00	Intercept for T _l and T _a linear regression
c1soil	-	PET	-1.50	1.50	Intercept for T _{soil} and T _a linear regression
K _{th}	Wm ⁻¹ °C ⁻¹	PET	0.50	1.50	Thermal conductivity for ground heat flux
D _{soil}	mm	PET	0.10	0.20	Effective soil depth for heat transfer
T _r	°C	PET	0.00	2.00	Threshold T _a for all precipitation as rain
T _s	°C	PET	-3.00	1.00	Threshold T _a for all precipitation as snow
dcf	d	PET	5.00	10.00	Albedo decay rates during melt
dc _s	d	PET	10.00	30.00	Albedo decay rates in cold conditions
albresd	mm	PET	10.00	30.00	Snowfall depth after which albs is reset
albi	-	PET	0.10	0.35	Land albedo
α	-	PET	1.10	1.40	Priestley-Taylor parameter
CX	mm°C ⁻¹ d ⁻¹	Snow	4.00	6.00	Degree day factor
CFR	-	Snow	0.00	0.10	Refreezing coefficient
TM	°C	Snow	-3.00	2.00	Threshold T _a for smelting
TX	°C	Snow	-3.00	2.00	T _a below which precipitation as snowfall
LW	-	Snow	0.05	0.10	Max. free water content in snow
s00	-	Snow	2.00	2.50	00 quantile in statistical snow distribution
s25	-	Snow	0.95	1.00	25 quantile in statistical snow distribution
s50	-	Snow	0.90	0.94	50 quantile in statistical snow distribution
s75	-	Snow	0.80	0.90	75 quantile in statistical snow distribution
s100	-	Snow	0.20	0.50	100 quantile in statistical snow distribution
h _{maxPer}	mm	RR	0.00	20.00	h _{max} for open and vegetation areas
h _{maxBu}	mm	RR	0.00	45.00	h _{max} for built-up areas
h _{maxImp}	mm	RR	0.00	45.00	h _{max} for impervious areas
h _{maxPET}	mm	RR	5.00	20.00	Max. h after which AET = PET
i _{cp}	mmh ⁻¹	RR	0.00	20.00	Max. infiltration capacity for open and vegetation areas
i _{cb}	mmh ⁻¹	RR	0.00	15.00	Max. infiltration capacity for built-up areas
SS _{max}	mm	RR	20.00	60.00	Max. soil storage capacity
GS _{max}	mm	RR	30.00	70.00	Max. groundwater storage capacity
m	-	RR	0.15	1.50	Soil pore-size index
θ _r	-	RR	0.00	0.15	Residual soil moisture content
n	-	RR	0.30	0.65	Soil porosity
K _{sat}	ms ⁻¹	RR	1.E-05	1.E-03	Saturated hydraulic conductivity
k _{soil}	s ⁻¹	RR	1.E-05	1.E-03	Coefficient for interflow IF
k _{gw}	s ⁻¹	RR	1.E-05	1.E-03	Coefficient for groundwater flow GF
P _{in}	-	RR	0.00	0.50	Net fraction of IF entering the sewer pipe

Table 2. The NSE performance measures for calibration and validation periods for events E1-E4, Summer-Autumn season (SA1) and part of Winter-Spring seasons (WS1 and WS2).

Calibration	Period	Validation					
		E1	E2	E3	E4	SA1	W
E1	01.08.1993 00:00- 01.08.1993 12:00	0.81	0.32	0.34	0.67	0.60	.
E2	28.09.1994-01.10.1994	-0.46	0.83	0.85	-0.21	0.50	.
E3	09.06.1995 00:00- 11.06.1995 00:00	-0.31	0.54	0.94	-0.08	0.67	.
E4	15.08.1998 12:00- 15.08.1998 20:00	0.38	0.19	0.64	0.87	0.60	.
SA1	01.06.1995-01.10.1995	0.23	0.48	0.81	0.31	0.76	.
WS1	10.01.1997-20.04.1997	-	-	-	-	-	0.
WS2	01.02.1998-08.03.1998	-	-	-	-	-	0.

Table 3. Summary of total volumes in mm over the whole catchment and percentages of fluxes for the calibration periods.

Description	E1	E2	E3	E4	SA1	WS1	W
P[mm]	18.70	50.30	30.50	16.70	238.30	566.80	237
Qobs*[mm]	4.36	29.65	11.64	-	-	-	160
IexsSF[mm]	1.29	10.36	4.50	3.24	7.54	208.55	47
SatexsSF[mm]	0.00	0.00	0.00	0.00	0.00	0.00	0.0
QTsurface = IexsSF + SatexsSF[mm]	1.29	10.36	4.50	3.24	7.54	208.55	47
ET = AE + AET[mm]	0.18	1.00	0.78	0.05	43.31	14.91	0.1
IF[mm]	14.38	39.29	21.89	10.08	187.85	356.50	167
GF[mm]	0.00	0.00	0.00	0.00	0.00	0.00	0.0
QTsubsurface = IF + GF[mm]	14.38	39.29	21.89	10.08	187.85	356.50	167
IFsewer[mm]	2.72	15.63	5.14	0.71	34.95	107.08	78
GFsewer[mm]	0.00	0.00	0.00	0.00	0.00	0.00	0.0
QTsubsurfacesewer = IFsewer + GFsewer[mm]	2.72	15.63	5.14	0.71	34.95	107.08	78
QT = QTsurface + QTsubsurface[mm]	15.67	49.65	26.39	13.32	195.39	565.06	215
Δ TotS** = P-ET-QT[mm]	2.85	-0.35	3.33	3.32	-0.40	-13.17	20
Qsim = QTsurface + QTsubsurfacesewer[mm]	4.01	25.99	9.64	3.95	42.49	320.24	126
ET/P[%]	0.94	1.98	2.56	0.32	18.18	2.63	0.1
Δ TotS**/P[%]	15.26	-0.69	10.91	19.91	-0.17	-2.32	8.4
QTsurface/P[%]	6.91	20.60	14.75	19.39	3.16	36.79	20
QTsubsurface/P[%]	76.89	78.11	71.77	60.38	78.83	62.90	70
QT/P[%]	83.80	98.71	86.52	79.77	81.99	99.69	90
QTsubsurfacesewer/P[%]	14.52	31.07	16.84	4.28	14.67	18.89	32
Qobs*/P[%]	23.32	58.94	38.17	-	-	-	67
Qsim/P[%]	21.44	51.67	31.59	23.67	17.83	56.50	53
Qsim/Qobs*[%]	91.92	87.66	82.76	-	-	-	78
Qsim/QT[%]	25.58	52.35	36.51	29.67	21.75	56.67	58
QTsurface/Qsim[%]	32.26	39.87	46.69	81.93	17.74	65.12	38
QTsubsurfacesewer/Qsim[%]	67.74	60.13	53.31	18.07	82.26	33.44	61

*Total volume of Qobs was estimated by filling the missing flow records by linear interpolation technique for calibration periods with small proportion of missing records (E1, E2, E3 and WS1).

** Δ TotS = change in total storage (surface depression or snow water equivalent, soil moisture and groundwater storages).

Figure 1. Location map, components of the stormwater drainage network and land use classes of the study catchment

Figure 2. The model structure for the runoff generation.

Figures 3. Plots of hydrographs of observed flow (Q_{obs}) and routed simulated flow (Q_{sim}), and some unrouted generated runoff fluxes for the event-based calibrations (a) E1, (b) E2, (c) E3 and (d) E4.

Figure 4. Plots of the simulated and observed flow hydrographs along with other variables related to the snow model for the seasonal calibrations (a) SA1, (b) WS1 and (c) WS2.

Figure 5. Plots of the dominant generated runoff fluxes (unrouted) (a) SA1, (b) WS1 and (c) WS2.

Figure 6. (a) Plots of mean flow travel times to the outlet (T_i) for the sub-catchments 1-54 and (b) Plots of typical STS response functions for the WS1 calibration for some sub-catchments.

